APPENDIX I

RADAR AND ACOUSTIC MONITORING SURVEYS

Natural
Forces

Westchester Wind Project – Radar and Acoustic Monitoring

Prepared for:

Natural Forces Developments Ltd.
108 Hollis Street, Suite 1205
Halifax, NS B3J 3N4

Project No. 105712-01

Prepared by:

Hemmera Envirochem Inc.
351 Prospect Ave.
Kentville, NS B4N 4R5
T: 778.669.0424
hemmera.com

February 9, 2022

TABLE OF CONTENTS

LIST OF FIGURES (WITHIN TEXT)

APPENDICES

1.0 INTRODUCTION

Natural Forces Developments LP (Natural Forces) retained Hemmera Envirochem Inc. (Hemmera), a wholly owned subsidiary of Ausenco Canada Inc. (Ausenco), to conduct spring and fall radar and acoustic monitoring of nocturnal migrating birds at the Westchester Wind Project (the Project). The Project is located approximately 63 kilometers (km) northwest (NW) of the Town of Truro, Nova Scotia (NS).

Natural Forces is proposing 16 potential turbine locations for the Project, but will only develop up to 12 turbine locations. The turbines will range in size from 4.2 to 6.2 megawatts (MW) each with a total Project nameplate capacity up to 50 MW. The final turbine model has not been selected for the Project. The range in turbine specifications being considered include a hub height between 100 and 131 meters (m), rotor diameter between 138 and 170 m, for a total turbine height (i.e., tip of blade) between 170 and 200 m above ground level (agl). The potential rotor swept area (RSA) of the turbines will range from 20 to 200 m agl.

The *Guide to Preparing an EA Registration Document for Wind Power Projects in Nova Scotia* (Nova Scotia Government 2021) specifies that avian radar studies are required for projects that include turbines greater than 150 m in height. Given that the Project turbine will have a maximum total height greater than 150 m, Natural Forces consulted with the Canadian Wildlife Service (CWS) and Nova Scotia Environment (NSE) regarding the development and implementation of an avian radar and acoustics study.

Hemmera, in partnership with Dr. Phil Taylor of Tabanid Consulting and Acadia University completed spring and fall avian radar and acoustic monitoring at the Project. This report provides a summary of those findings.

1.1 Project Location

The location of the radar and acoustic equipment was chosen based on availability of participating landowners to host the radar, access throughout the Project area, site security and clear sight lines. The radar was located approximately 1.5 km from the nearest turbine and sited on private land adjacent to a summer residence of a participating landowner (See **Figure 1.1**). At that distance, the radar data provides sufficient representation of the movement of nocturnal migrants over the Project area.

The acoustic sensors were placed near the radar location and throughout the Project area (See **Figure 1.1**). This distribution of sensors also allows for sampling of nocturnal migrants throughout the Project area.

Natural Forces
Westchester Mountain Wind Project

Project Area

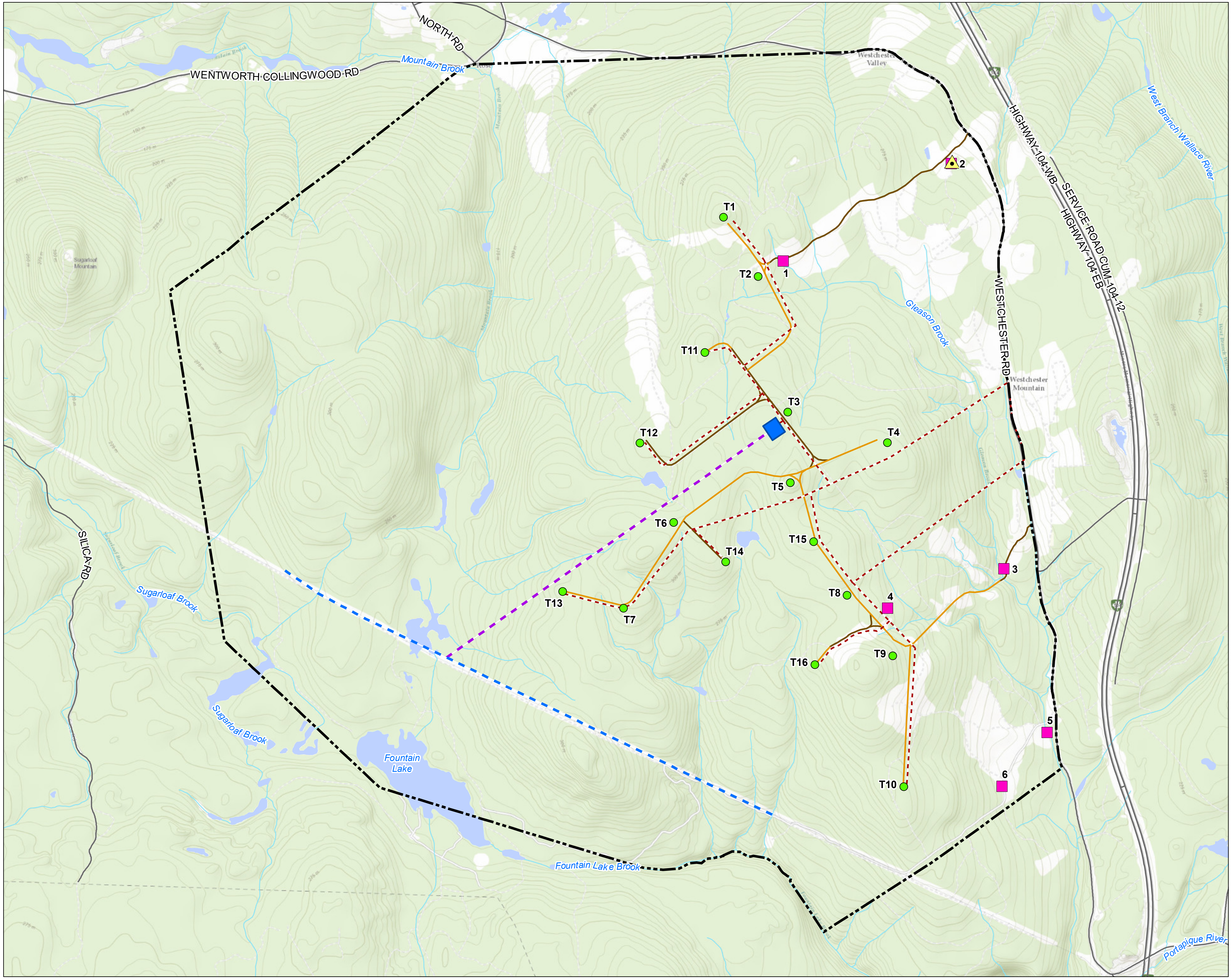

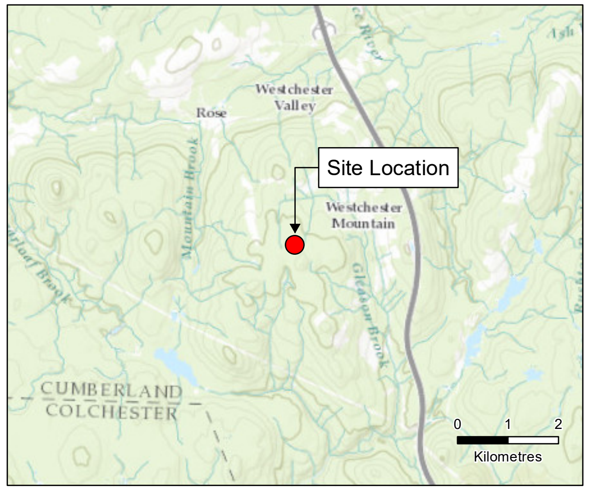

Legend

- 🟪 Audio Sensor Location
- ⚠ Radar Location
- ● Turbine Location
- Collector Line
- Existing Road
- New Road
- Existing Transmission Line
- Project Transmission Line
- Local Assessment Area
- 🟦 Substation
- Road
- Watercourse
- Waterbody

Notes

1. Natural Forces is proposing 16 potential turbine locations for the Project, but will only develop up to 12 turbine locations.
2. All mapped features are approximate and should be used for discussion purposes only.
3. This map is not intended to be a "stand-alone" document, but a visual aid of the information contained within the referenced Report. It is intended to be used in conjunction with the scope of services and limitations described therein.

Sources

- Contains information licensed under the Open Government Licence(s) - Nova Scotia
- Aerial Image: ESRI World Topographic Map
- Inset Basemap: ESRI World Topographic Map

N

1:25,000

0 200 400 600 800 1,000
Metres

NAD 1983 UTM Zone 20N

Page Size: 11" x 17"

105712-01	Production Date: Feb 9, 2022	Figure 1

Hemmera An Ausenco Company
natural forces

Path: S:\Geomatics\Projects\105712\01\mxd\Fig1__105712_01_SiteLocation_220119.mxd

2.0 METHODS

The following section provides a summary of the methodology used to collect and analyse the radar and acoustic data.

2.1 Radar Monitoring

The radar system used to monitor both the spring and fall migration seasons has been used in the past to assess migratory bird movements at proposed wind energy projects in NS and New Brunswick (NB) (e.g., Burchill Wind Project [Taylor et al. 2020], Benjamins Mill Wind Project [Hemmera 2021]) and has been proven to provide an adequate representation of bird passage rates and heights. Further, the radar and acoustic monitoring system used on this Project was initially developed through federal (i.e., CWS) grant funding and has been improved upon through multiple iterations over the past 15 years. The approach used has been implemented on no fewer than four wind energy projects in NB and four energy projects in NS, along with two successful Master of Science degrees and presented in peer reviewed scientific publications. The radar system is described in detail below.

2.1.1 Spring Migratory Season

A Furuno (Camas, Washington, USA) 1962 BB marine radar operating in the microwave X-band (9410 ± 30 Megahertz (MHz), 25 kilowatt (kW)) with a 6-foot XN13A open-array antenna (with a beam width of approximately 22° in the horizontal plane and approximately 1.35° in the vertical plane) was deployed at the site for the spring season. The radar was mounted on a custom support framework in a vertical orientation to monitor the altitude of targets and was run in short pulse mode (2100 pulses per second) at 24 revolutions per minute (rpm).

This radar unit has a shorter range (compared to the unit used in the fall) with an approximate maximum range of detection for small birds (e.g., sparrows and warblers) of 800 m. The output from the radar was processed using a digitizing card (Sigma Sd, Rutter Technologies Inc., NL) and recorded using radR, an open source, R-based platform (Equipment www.radr-project.org, Taylor et al. 2010). All data (date, time, and location in space) on targets detected by the radar were stored in digital files for later processing (see Taylor et al. 2010 for details).

During the spring migration season, monitoring occurred from May 4 to June 6, 2021. During the 34-day monitoring period, the radar functioned properly for approximately 83% of the time (28 of 34 nights). Acoustic sensors were operational throughout the period.

2.1.1.1 Radar Data Processing

All recorded digital files were filtered to remove signal clutter (e.g., backscatter from surrounding vegetation) using program radR. Targets visually assessed to behave like birds (e.g., where multiple detections of a target moving in a particular direction) were identified to determine a ‘size’ threshold for target inclusion and then run through the tracking algorithm in radR to extract ‘tracks’ which represented multiple detections of the same target. Tracks were later filtered to include only those between 50 and 800 m altitude for use in figure presentations and analysis.

The power output of the spring radar was less comparative to the fall radar, resulting in fewer detections of small targets at larger distances. However, by examining the pattern of detection across nights, it was clear that the spring radar was consistently detecting targets below approximately 400 m agl. Thus, for the spring radar analysis we focused on the airspace between 100 and 400 m agl, which encompasses the airspace of the turbines plus an additional 200 m. These data were further summarized by grouping into altitude (100 m bins) and time (30 min bins) and plotted.

2.1.2 Fall Migratory Season

A Furuno 8252 marine radar with the same specifications and operational parameters as the spring was deployed at the site for the fall season. The approximate maximum range of detection for small birds (e.g., warblers and sparrows) was 1,000 m with the same beam width on the horizontal and vertical plane as used in the spring.

Prior to the fall deployment, the radar was ‘calibrated’ while in a horizontal orientation using targets at a known distance. The radar signal was digitized at 4.5 m range resolution with an azimuth resolution of 1.35° using a DSPNOR ScanStreamer (Bergen, Norway). Data were saved onto external hard drives and later analyzed using Cognitive Marine Tracker (CMT) radar analysis software, from the Cognitive Radar Corporation (Waterloo, Ontario).

Monitoring was completed from August 10 to October 31, 2021. The radar functioned for 82 of the total 83 nights during this time period (99% of the time).

2.1.2.1 Radar Data Processing

Targets were extracted over background noise if they were at least 6 pixels in size, and the sensitivity to detect targets over the threshold in the CMT software (Pfa setting) was set at 0.02. These settings allowed for weak targets at long range to be identified over background noise, but also were sensitive enough to pick up insects at short range and birds at the edge of the radar beam. To filter out insects and birds on the periphery of the beam at close range, the peak power of the radar return for each target (“peak_val setting”) was used and corrected for range, since returned power decreases with range to the fourth power (“scaled intensity”). The numbers of targets in five-minute intervals across the entire season were then correlated with acoustic data, to determine a threshold above which we could be more confident targets were primarily birds. The correlation between acoustic and radar detections plateaued at a scale intensity of 5, so targets below that threshold were removed from the analysis.

Radar data was visually inspected to determine periods of rain, which were excluded from analysis. Targets below 70 m agl were also eliminated because they are contaminated by ground clutter.

Targets were then extracted from a “column” of air starting at a distance along the ground between 300 m and 320 m from the radar. This approach allows for smaller birds to be detected at high altitudes, while sampling low altitudes horizontally from the radar.

2.2 Acoustic Monitoring

Two types of acoustic monitoring devices were used to detect nocturnal flight calls (NFCs) of migratory birds (primarily passerines) at the Project area.

A 21c microphone system (Old Bird) (Old Bird Inc., Ithaca, New York, USA) was deployed in proximity to the radar and connected to a secondary booster amplifier and power supply. Audio was recorded with a raspberry Pi3B (spring) or an iSound Recorder 7 (Abyss Media) (fall) and saved onto external hard drives. The microphone was programmed to start recording up to an hour prior to sunset, and to stop after sunrise.

In addition, a network of 6 acoustic sensors (Audiomoths™) were deployed across the Project area to record NFCs (see **Figure 1.1**). These sensors were programmed to begin recording approximately one hour before the end of evening civil twilight and finish recording one hour after the beginning of morning civil twilight and placed in open areas with a clear view of the sky. The sensors were checked approximately every 14 days to replace batteries and download data onto an external hard drive. In the spring these sensors ran continuously between dusk and dawn; in the fall they were programmed to sample alternate 10 min periods.

The detection range of each recording unit is estimated to be up to 200 m or more for the Old Bird system (the type of unit located adjacent to the radar) and approximately 100 m for the Audiomoth sensors (the units located throughout the Project area).

2.3 Data Analysis

All analyses were conducted using program R (R Statistical Core team; V 3.52).

2.3.1 Visualization patterns

All radar and acoustic detections were plotted to visually explore the patterns of bird movement at the site in conjunction with wind direction and strength at the ground level and aloft. Analysis within this report is restricted to a summary of those observations.

Six nights from spring and 12 nights from fall that had large numbers of targets showing different patterns of bird behaviour at the site were visualized. The full set of visualizations for the spring and fall data are presented in **Appendix A**.

2.3.2 Radar Analysis

The primary objective of the radar study was to describe the general patterns of migrating birds at the site through visualizations, and statistically assess how the number of targets observed below 200 m in altitude relate to those above 200 m, and how the total number of targets observed relate to particular weather variables of interest.

Two response variables were derived from the compiled radar data. The first was the number of targets detected in each hourly period (excluding rain) across all nights. The second was the ratio of the number of targets detected below and above 200 m in altitude. That ratio is positively related to the proportion of targets flying beneath 200 m but does not represent the actual proportion, since the probability of detecting targets decreases with increasing altitude due to changes in the shape and size of the radar beam, and the size of the targets. As such, this ratio overestimates the proportion of targets observed at lower altitudes to some unknown extent. Furthermore, because the sensitivity of the radar in the spring was less than the fall, these absolute values are not comparable across seasons. Regardless, the pattern of how the ratio changes with the volume of targets detected, is informative; **the ratio serves as a useful indicator to determine under which conditions and times more targets are flying at relatively lower altitudes**.

Weather data (wind speed and direction, pressure, temperature, and humidity) were acquired from the National Centers for Environmental Prediction (NCEP) (https://www.weather.gov/ncep/) and downloaded via the RNCP package in program R (R Statistical Core Team V 3.02). Surface and upper altitude weather data were interpolated for the location of the radar at the surface, and for wind data, at three additional pressure levels (altitudes approximating 140 m, 792 m and 1,492 m). For this report, wind data from the surface and 792 m altitude were used.

For both seasons, the effect of weather (tailwind assistance, barometric pressure, change in barometric pressure and humidity) on a) the log of the number of targets detected and b) the proportion of targets below 200 m (relative to above 200 m) was modelled using generalized linear models. Model support was assessed using Akaike's Information Criterion (package MuMIn; Barton 2012).

The relationship between targets aloft and weather is complex and nonlinear, and as such, statistical models of such relationships can be difficult to interpret. Therefore, simple models were fit to show the dominant relationships between the two response variables described above and the weather variables. Furthermore, since relationships between wind speed, wind direction and the number of birds aloft can also be complex, a 'tailwind assistance' variable was used to provide a measure of how much the wind would assist a given bird flying in a specific direction. It is known that nocturnal migrants fly with positive tailwind assistance (Peckford and Taylor 2008). Tailwind assistance was calculated using an assumed direction of 225 degrees (see Peckford and Taylor 2008) for fall, and 45 degrees for spring. Thus, for the fall, if the wind was flowing from the direction of 225 degrees, then the birds' tailwind assistance would be negative (a headwind); if the wind was flowing towards 225 degrees, the birds' tailwind assistance would be positive. The strength of the assistance is a function of both the direction of the wind, and its speed.

In addition to the weather variables described above, terms were fit for month of the year and time of night (categorized into 'sunset', 'sunrise' and 'middle' of the night, with 'sunset' being 90 minutes after the end of evening civil twilight, 'sunrise' being 90 minutes before the beginning of morning civil twilight, and 'middle' representing the remainder of the night). These variables help assess how total numbers differed at migratory initiation (sunset), cessation (sunrise) and during the night, as well as how numbers differed with time of year (a potential measure of species composition).

The R package 'tidyverse' (Wickham et al. 2019) was used for data manipulation and visualization and the function 'glmer' in package 'lme4' (Bates et al. 2015) was used for statistical modelling. In all cases, mixed effects models were fit, with the day of the year as a random effect. Treating day as a random effect allows the model to account for additional variation in counts that is not fully captured by the weather or timing variables. Models of the total counts were fitted with a 'poisson' family (i.e., the relationship between the response and the predictor variables was on a log scale) and measure of the proportions were filled using a 'binomial' family, which transforms the response using a log-odds ratio. Model fits were assessed by examining residual plots.

2.3.3 Acoustic Data Processing

All acoustic data were either sampled or resampled to 22 kilohertz (kHz) (the frequency range where most NFCs occur), then clipped to encompass only the period of time between the end of evening civil twilight and the beginning of morning civil twilight. It is during this period that birds make NFCs while actively migrating (Evans 2005).

All acoustic files were processed using custom-built night flight call detectors developed using the OpenSoundScape program (www.opensoundscape.org). A library of approximately 50,000 identified groups of calls (groups modified from Sanders and Mennill, Appendix 1) were used to train a convolutional neural network model which was used to classify the recordings. The classifier assigns a 'score' to each species (or group), which is related to the probability that the detection is actually that species. These results were then visually examined to identify a threshold where approximately 85% certainty was obtained that the identity was correct. For ease of presentation and interpretation of the data, the classifications were then amalgamated into two larger groups (sparrows and warblers).

Summaries of the acoustic data obtained from the Old Bird and Audiomoth microphones are presented for all nights for which data was collected in the spring and fall.

3.0 RESULTS

3.1 Spring

3.1.1 Nocturnal Migration Patterns

Active migration was observed on multiple nights during the spring migration season. The peaks in number of radar targets detected varied with altitude (**Figure 3.1)**.

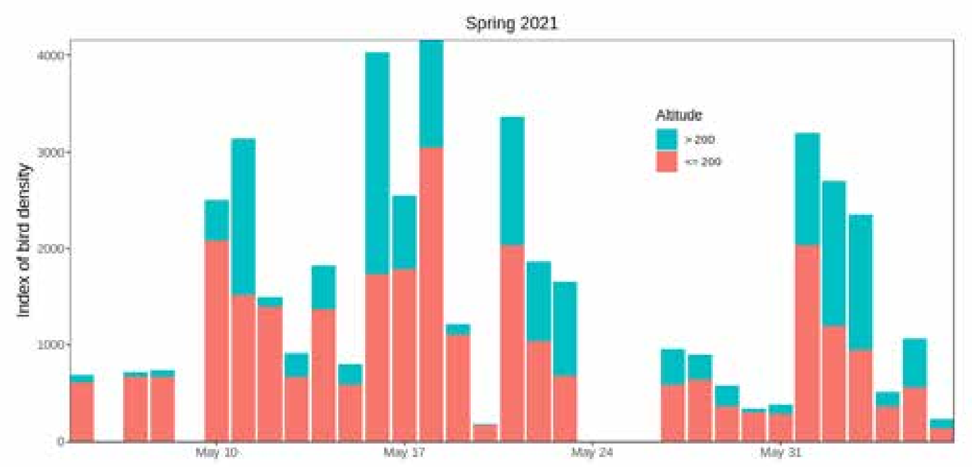

Figure 3.1 Radar Detections by Altitude during Spring 2021

Figure 3.2 shows the altitudinal, seasonal, and within night distribution of radar targets for select nights in the spring. These nights were selected for visualization as they represented nights where high volumes, or different types of migratory activity was observed. The entire data set of nights for the spring season can be found in the **Appendix A**.

Each plot within **Figure 3.2** is a separate night, with the beginning and end of civil twilight indicated by the vertical green and yellow lines, respectively. Date and time are on the x-axis and altitude is on the y-axis. Hexagonal points are radar detections divided into time and altitude bins and are scaled from light grey (few detections) through dark purple to yellow (many detections). Wind direction and strength at the surface (red arrow) and aloft (792 m; green arrow) for each hour are displayed at the top of each plot. Red lines represent the approximate altitudinal range of the RSA.

Acoustic detections (a single NFC) are red points along the base of each plot. Note that detections are more frequent when the radar shows targets at lower altitudes and that the detection range of each recording unit is estimated to be 100 m for the Audiomoth sensors and 200 m or more for the Old Bird system. Also, it should be noted that some species migrate without calling (e.g., vireos and flycatchers), so the number of radar targets will not always correlate with the number of acoustic detections. This is illustrated in **Figure 3.2** where large number of low altitude radar detections and acoustic detections were both observed on May 7 and 18, while on June 2 large numbers of acoustic detections did not correspond with the large number of low altitude radar detections. A pattern of very low altitude detections at some nights at sunset and sunrise were determined through visualizations of flight patterns are American woodcock display flights (see May 7 for example). Those targets were not removed from the dataset.

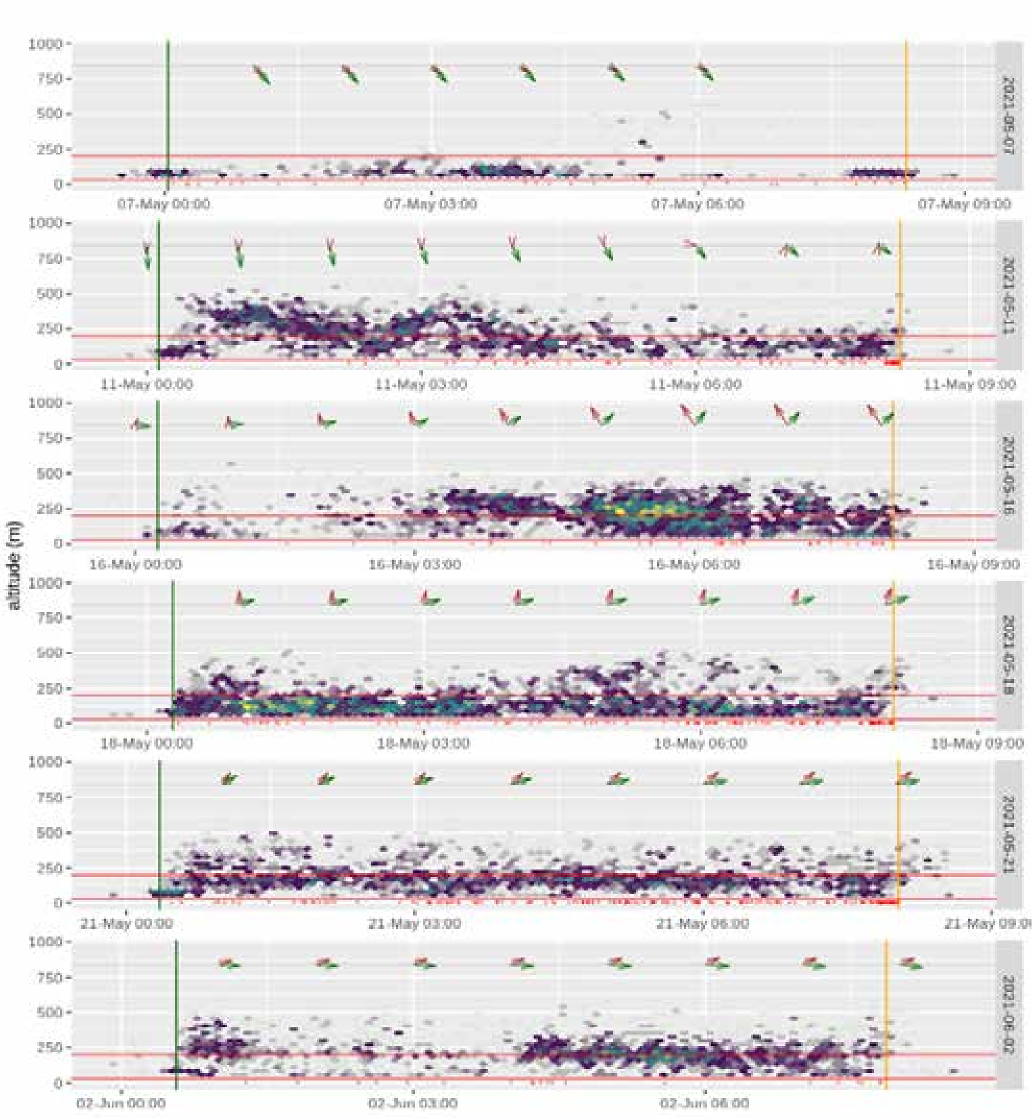

Figure 3.2 Radar and acoustic detections and wind conditions on select nights in spring 2021

3.1.2 Nocturnal Flight Call Detections

Flight calls were summarized for same select nights in the spring as displayed in **Figure 3.2** and grouped into ‘Warblers’ and ‘Sparrows’ species groups. **Figure 3.3** shows the pattern of NFC detections for each species group during the spring. Within **Figure 3.3** each dot represents a single NFC detection (Old Bird and Audiomoth recording units combined). During the spring we see the expected pattern of more warblers detected during the latter part of the season (e.g., the night of May 21).

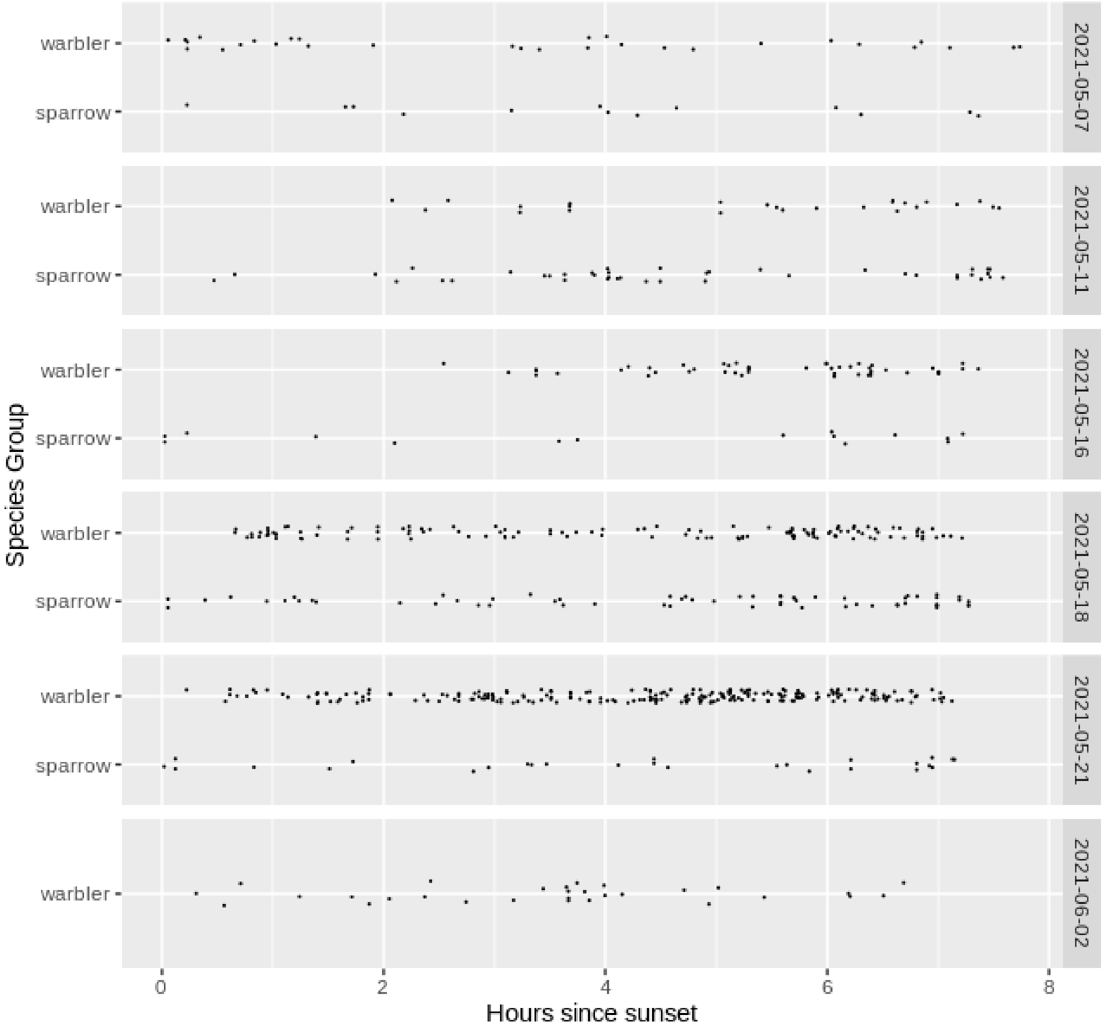

Figure 3.3 **Nocturnal Flight Calls Detected by Species Group during Six Select Nights during Spring 2021**

3.1.3 Altitudinal distribution of radar targets

Across all nights, the number of targets generally decreased with increasing altitude (**Figure 3.4**). Most targets observed were at lower altitudes. The number of targets detected begins to decline sharply above approximately 300 m; this decline is partly due to an actual decrease in the number of birds, but also reflects the declining probability of detecting birds at more distant ranges. It is difficult to separate the effects of these two variables. Also, the data show a peak in detections at the lowest possible bin (i.e., 70 m to 95 m); however, at that height there is a greater likelihood of data being contaminated with insects and ground clutter. The red line shown in **Figure 3.4** represents the maximum potential height of the turbines.

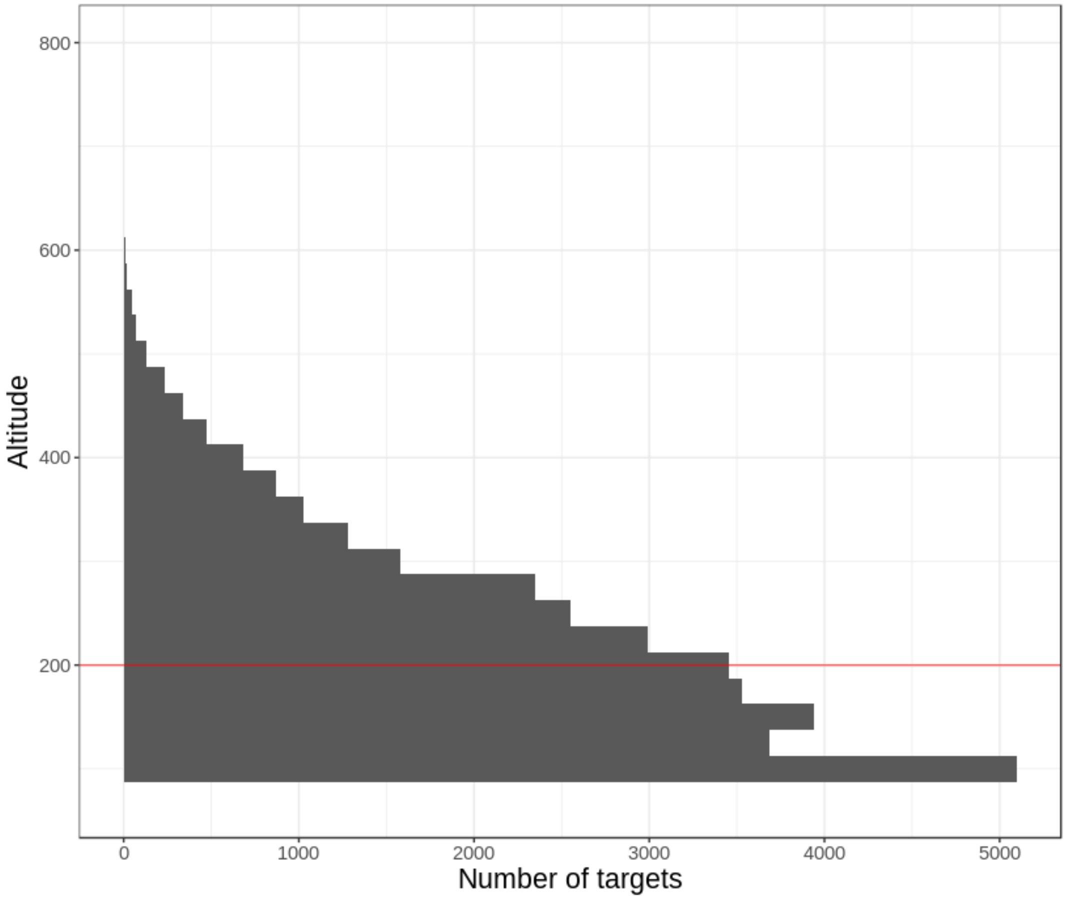

Figure 3.4 Number of Radar Targets Detected by Altitude for Spring 2021

Figure 3.5 shows the density of radar detections by altitude for six selected nights in spring that contained the most migration. Each night is presented with a different density scale, to emphasize the pattern instead of the actual number of detections. The red line indicates the maximum height of the turbines.

The pattern of detection of targets by altitude varied across nights. On some nights (e.g., May 18 and May 21) large numbers of targets are detected below the maximum RSA, whereas on other nights (e.g., May 16 and June 2) the opposite pattern is observed.

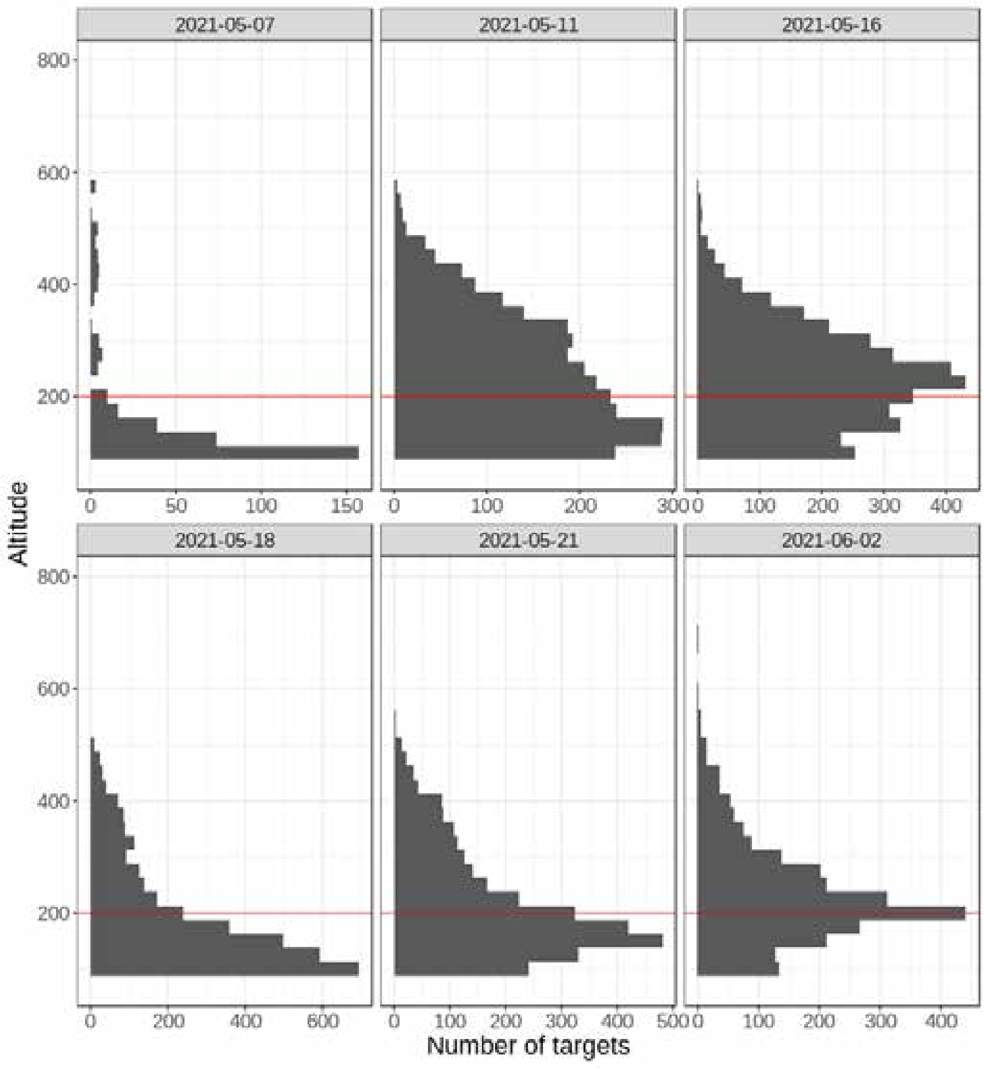

Figure 3.5 Number of Radar Targets by Altitude for Six Select Nights during Spring 2021

3.1.4 Statistical Analysis of Spring Radar Data

Statistical models provided evidence that the total number of birds per hour was related to tailwind assistance (at ‘surface’), time of night (sunset, sunrise, and middle of the night) and weather (temperature, surface pressure and relative humidity). The most important differences are summarized in **Figure 3.6** and can be attributed to different behaviours through the night. The radar detected numerous targets immediately after the initiation of migration (take-off after sunset) and during the middle of the night (continued migration), and fewer in the morning. That the period immediately before dawn sees many fewer targets may reflect that birds are either not landing within the Project area following migration or they are consistently ending their migration flights early in the night (also see **Appendix A**).

Within **Figure 3.6** each point represents the number of targets in hourly bins, classified by time periods (panels) and month (colours). Tailwind speeds are plotted along the x-axis in km per hour with negative and positive values representing tailwind assistance. To improve data visualization, the total number of targets is represented on the y-axis by taking the log base 10 of the number of targets in hourly bins. The lines are locally weighted regressions for each group, showing a positive relationship for the bulk of the night during May and a negative relationship on the small number of nights in June.

The number of targets detected is low in strong headwinds (negative tailwind assistance), high with light through moderate tailwinds, and low again in very strong tailwinds. In June few birds were detected on nights with very strong tailwinds **Figure 3.6**. This follows a general pattern that birds prefer to migrate with tailwinds or very light headwinds (e.g., Peckford 2006).

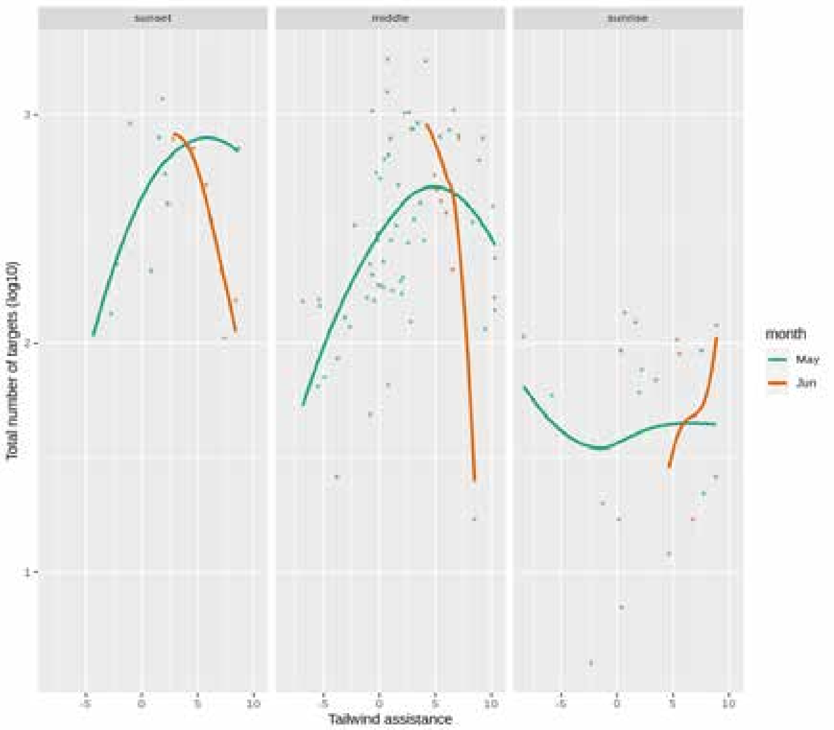

Figure 3.6 **The Relationship Between Tailwind Assistance on Total Number of Targets Across Time of Night and Months for Spring 2021**

Relative number of birds at lower altitudes

The index of the proportion of targets flying at low altitudes demonstrates the proportion of targets below a given altitude (i.e., 200 m) in relation to what is detected above that altitude. The index was related to the overall number of migrants, as well as all timing and weather variables. The value of tailwind assistance at approximately 792 m provided a better fit that more strongly expressed the relationship between data points than tailwind assistance at lower altitudes in this model.

In **Figure 3.7**, each dot represents the number of birds detected below 200 m divided by the total number of birds observed, in each hourly bin, classified by time of night. The lines are smoothed relationships between the index, and the total number of targets are presented on a log scale.

The primary finding expressed in **Figure 3.7** is that on nights when large numbers of targets were detected (e.g., during the beginning and middle of the night) there tended to be fewer of those targets at lower altitudes. The different pattern in the 'sunrise' time of night parameter is related to the low number of targets observed during that time of night.

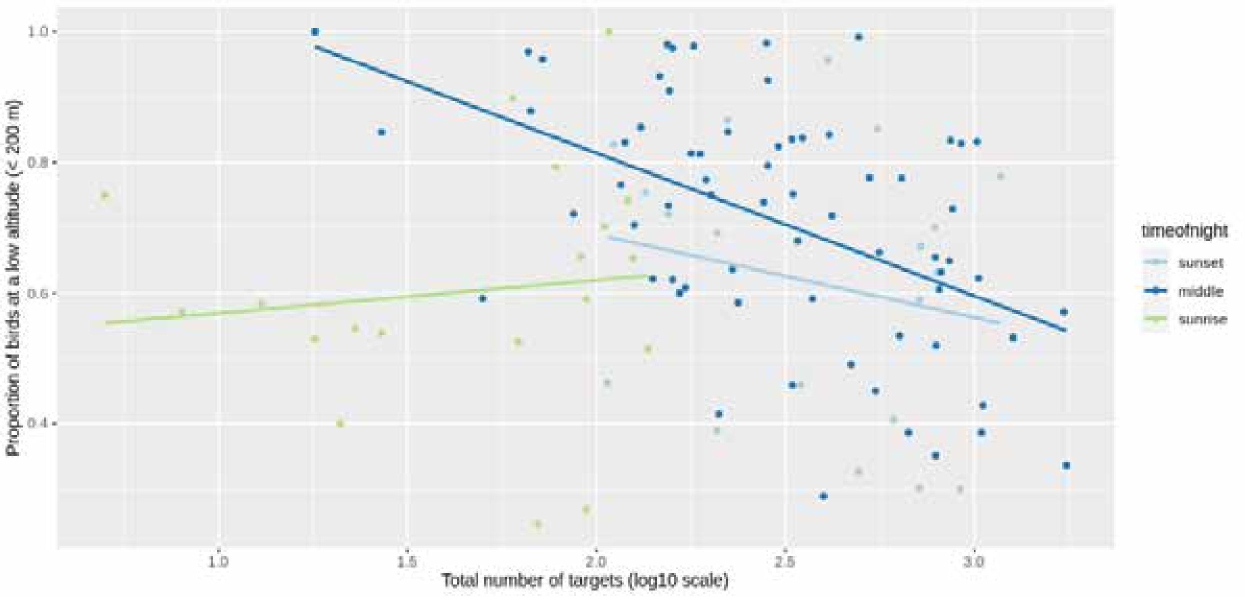

Figure 3.7 **Proportion of Targets at Low Altitude in Comparison to Total Number of Targets at Three Time Periods in Spring 2021.**

3.2 Fall

3.2.1 Nocturnal Migration Patterns

During the fall the majority of migration occurred on relatively few nights, with peaks on August 9, September 17 and October 9. The peaks in number of radar targets detected varied with altitude (**Figure 3.8**).Error! Reference source not found.

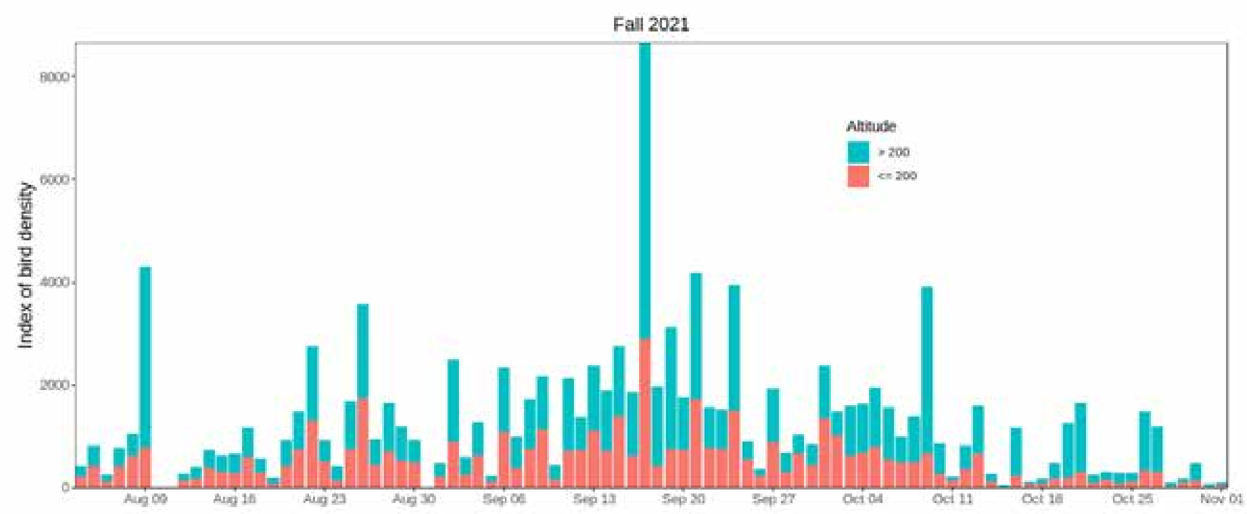

Figure 3.8 Radar Detections by Altitude during Fall 2021

Figure 3.9 and **Figure 3.10** shows the altitudinal, seasonal, and within night distribution of radar targets for select nights in fall, 2021. These nights were selected for closer analysis as they represented nights where high migratory activity was observed. The entire data set of nights for the spring and fall 2021 seasons can be found in **Appendix A**. The blue boxes shown in **Figure 3.9** and **Figure 3.10** represents a period of rain when raindrops and bird detections can not be distinguished. The remaining elements of **Figure 3.9** and **Figure 3.10** are the same as **Figure 3.2** and described above in **Section 3.1.1**.

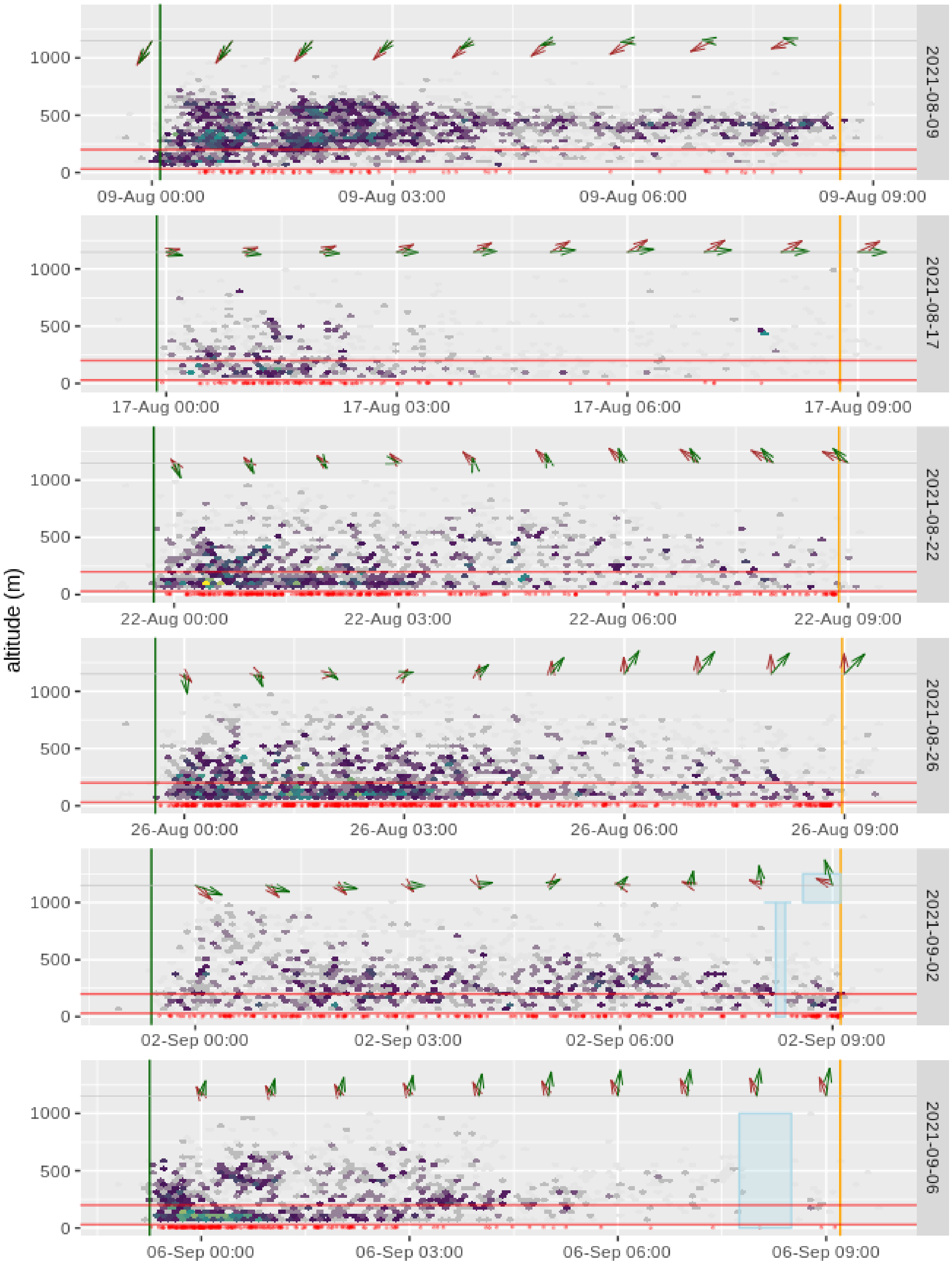

Figure 3.9 **Radar and Acoustic Detections and Wind Conditions on Six Select Nights in Early Fall 2021.**

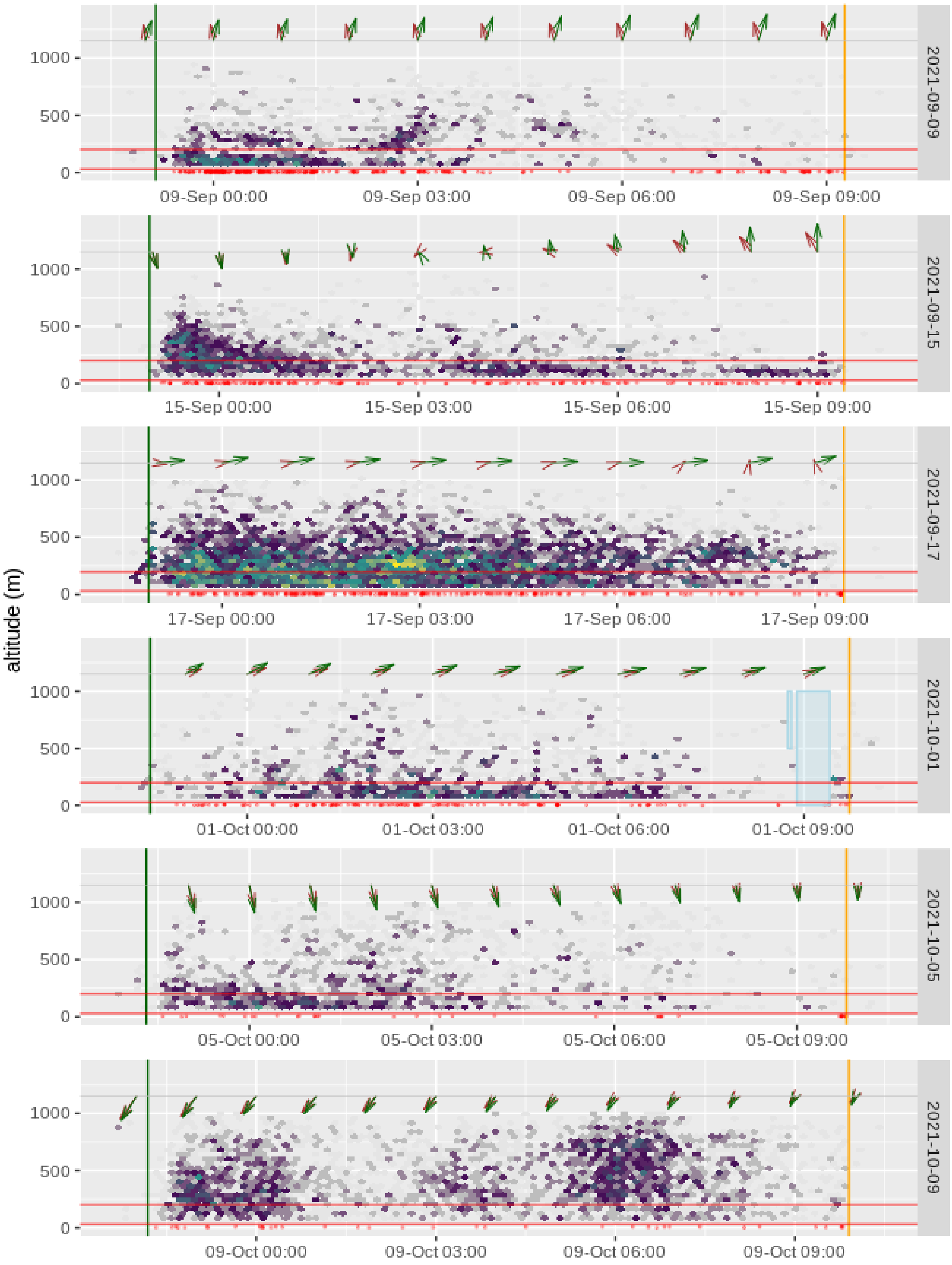

Figure 3.10 **Radar and Acoustic Detections and Wind Conditions on Six Select Nights in Late Fall 2021.**

3.2.2 Nocturnal Flight Call Detections

Flight calls were summarized for same select nights in the fall as shown in **Figure 3.9** and **Figure 3.10** above and grouped into 'Warblers' and 'Sparrows' species groups. Within **Figure 3.10** each dot represents a NFC detection. In **Figure 3.10** we see the expected pattern of warbler activity generally decreasing after mid-September.

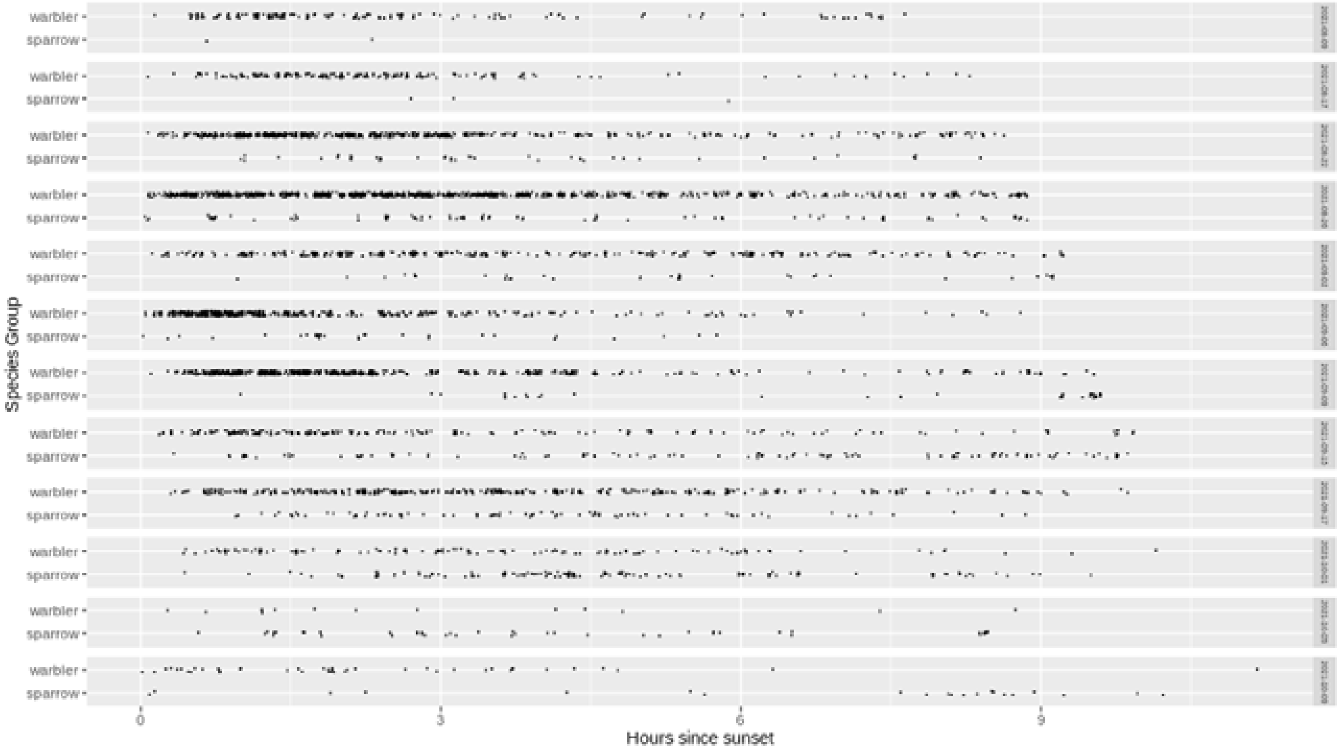

Figure 3.11 Nocturnal Flight Calls Detected during Select Fall Nights by Species Group

3.2.3 Altitudinal distribution of radar targets

Across all nights, the number of targets generally decreased with increasing altitude (**Figure 3.12**). The number of targets detected begins to decline sharply above approximately 400 m; this decline is partly due to an actual decrease in the number of birds, but also reflects the declining probability of detecting birds at more distant ranges. It is difficult to separate the effects of these two variables. Also, the data show a peak in detections at the lowest possible bin (i.e., 70 m to 95 m); however, at that height there is a greater likelihood of data being contaminated with insects and ground clutter. The red line shown in **Figure 3.12** represents the maximum potential height of the turbines.

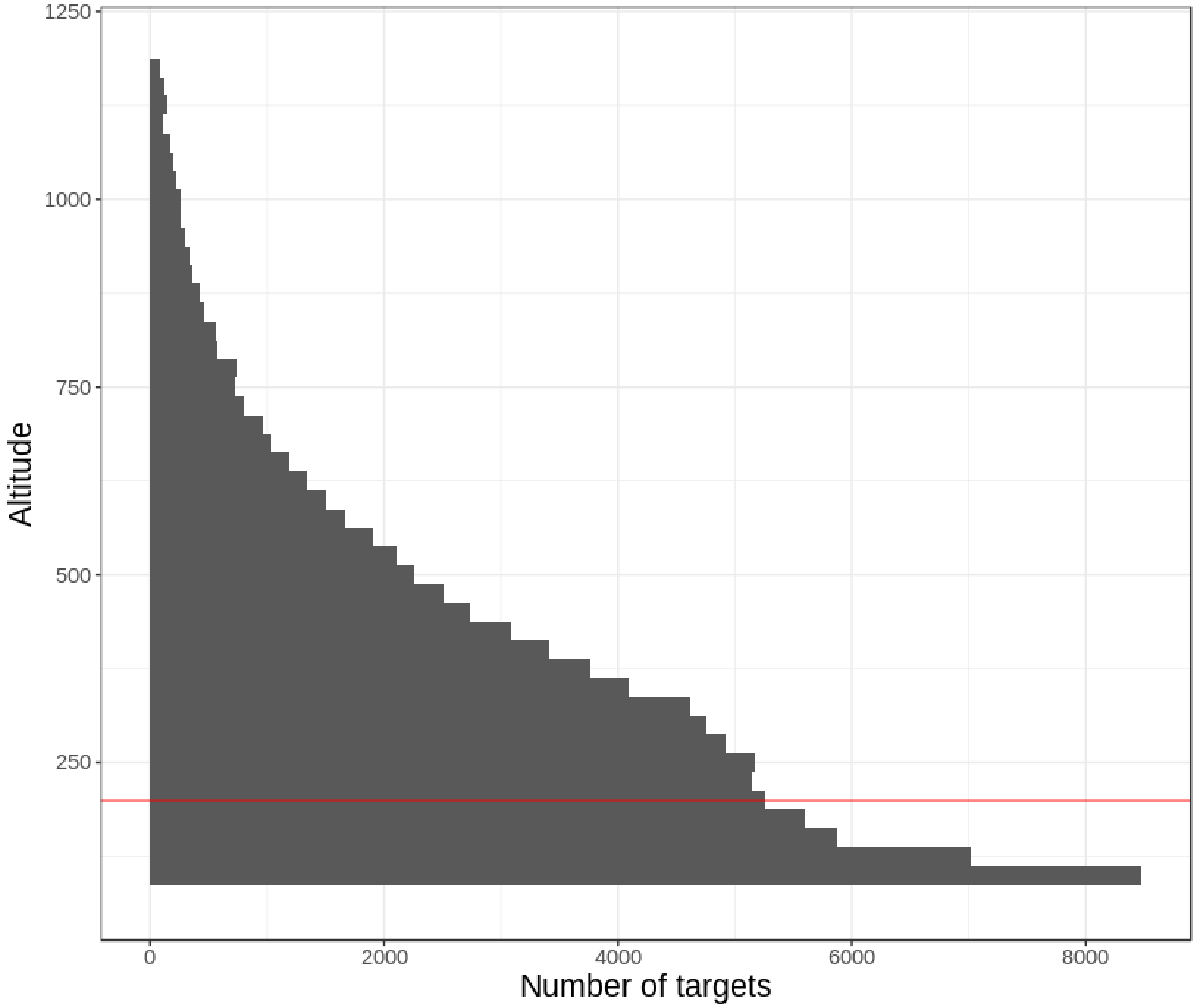

Figure 3.12 Number of Radar Targets Detected by Altitude for Fall 2021

Figure 3.13 shows the density of radar detections by altitude for the twelve selected nights in the fall that contained the most migration. Each night is presented with a different density scale, to emphasize the pattern instead of the actual number of detections. Note that the decline in detections above about 400 m is due to both a declining probability of detection, and fewer birds. The red line indicates the maximum height of the turbines.

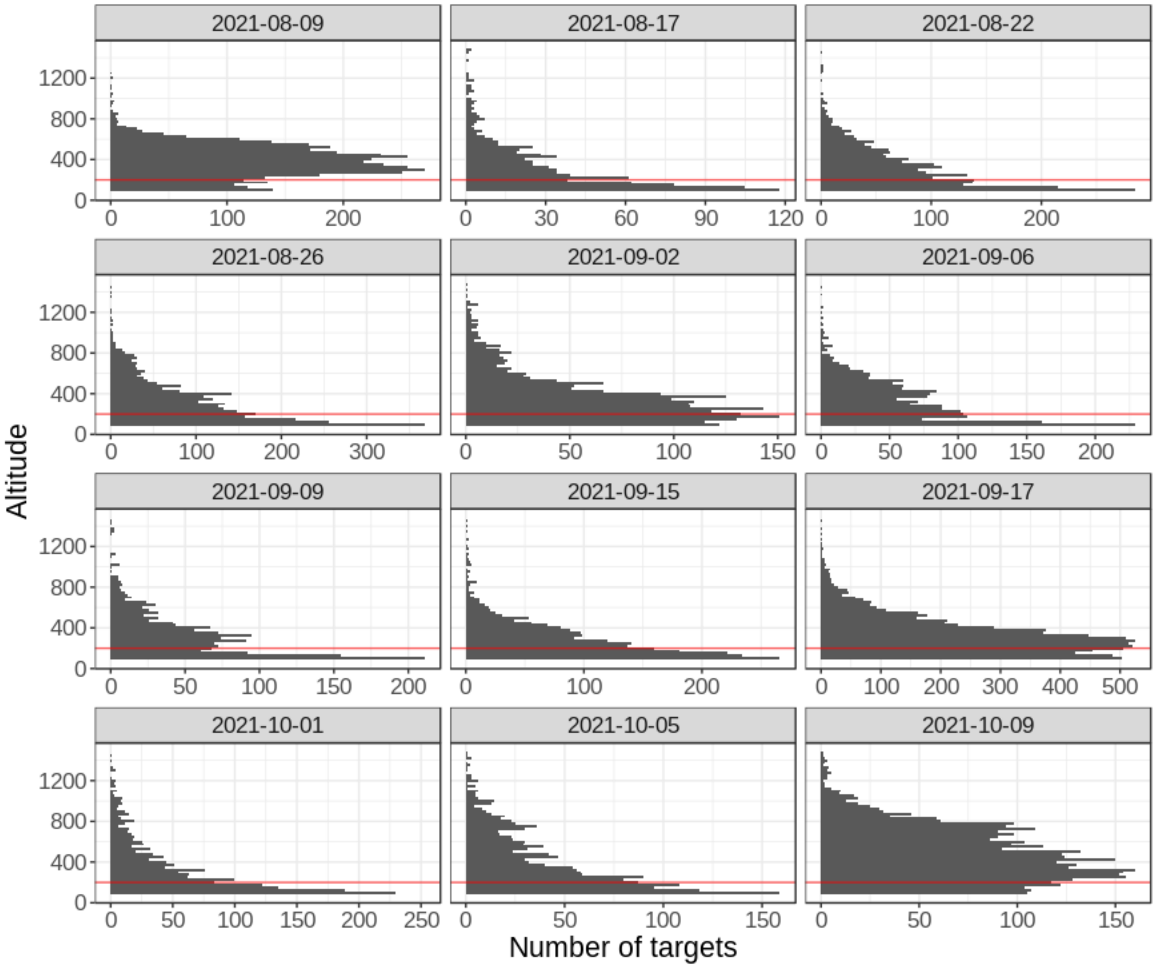

Figure 3.13 **Number of Radar Targets by Altitude for Twelve Select Nights During Fall 2021**

When focusing on the nights when most migration occurred, some nights show that the greatest relative density of migration occurred above the highest potential turbine RSA (e.g., August 9, September 2 and 17, and October 9) but on some high intensity migration nights (e.g., August 17, 22 and 26, and September 6 and 15) the greatest relative density of targets were within the RSA (**Figure 3.13**)

3.2.4 Statistical Analysis of Fall Radar Data

Total numbers of birds

Statistical models provided evidence that the total number of birds per hour was related to tailwind assistance (at 790 m), time of night (sunset, sunrise and middle of the night) and weather (temperature, surface pressure and relative humidity). The most important differences are summarized in **Figure 3.14** and can be attributed to different behaviours through the night. The radar detected numerous targets immediately after the initiation of migration (take-off after sunset) and during the middle of the night (continued migration), and fewer in the morning. August and September have the highest average number of targets, followed by October. That the period immediately before dawn sees many fewer targets likely reflects that birds are either not landing within the Project area following migration or they are consistently ending their migration flights early in the night (also see **Figure 3.9** and **Appendix A**). The same pattern was observed during the spring.

Within **Figure 3.14** each point represents the number of targets in hourly bins, classified by time periods (panels) and month (colours). The lines are linear regressions for each group, showing a positive relationship for the bulk of the night. During time periods with the largest numbers of targets there is a narrow range of tailwind assistance.

The number of targets detected is low in strong headwinds (negative tailwind assistance), high with light through moderate tailwinds, and low again in very strong tailwinds. During October in particular, few birds were detected on nights with very strong tailwinds (**Figure 3.14**). This follows a general pattern that birds prefer to migrate with tailwinds or very light headwinds (e.g., Peckford 2006).

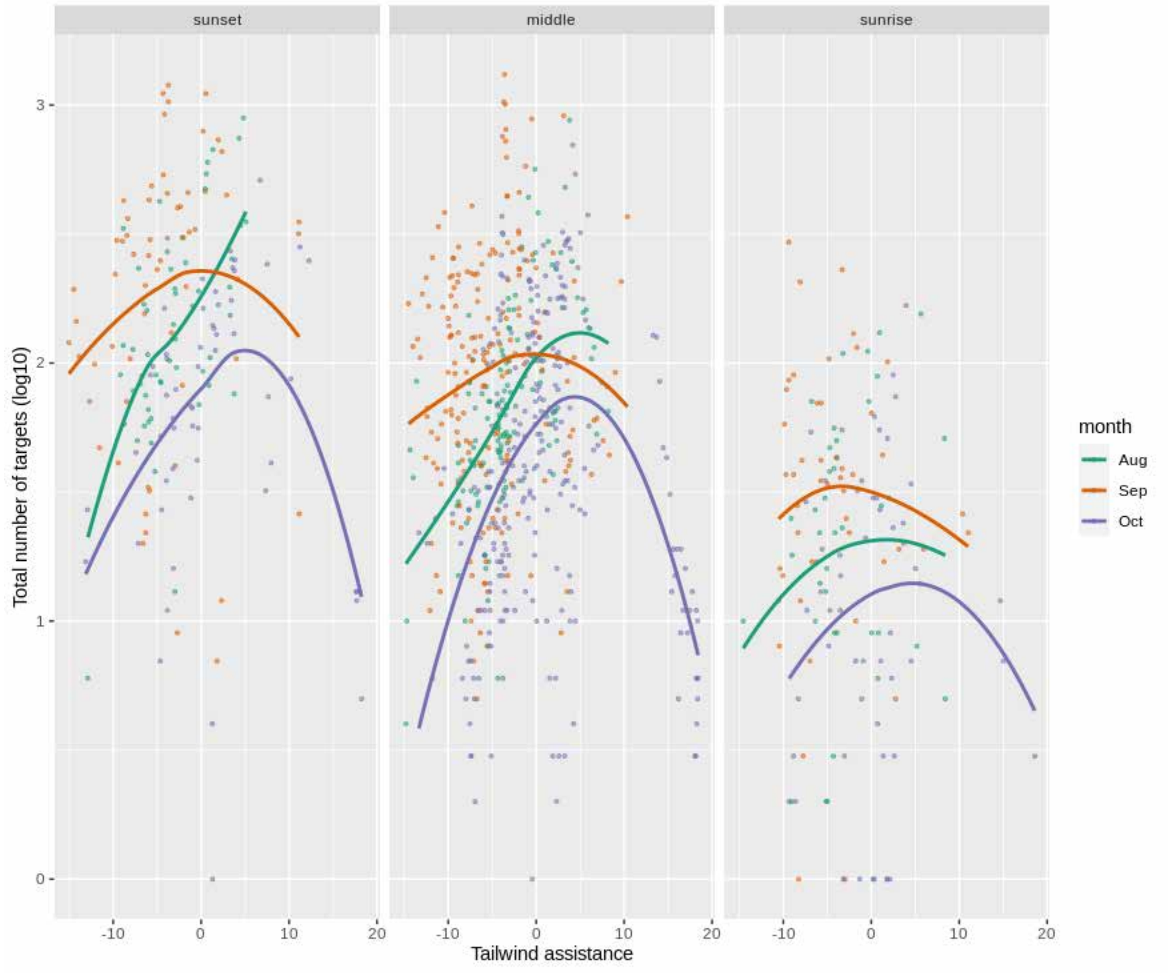

Figure 3.14 The Relationship Between Tailwind Assistance and Total Number of Targets Across Time of Night and Month for Fall 2021

Relative number of birds at lower altitudes

The index of the proportion of targets flying at low altitudes was related to the overall number of migrants, surface temperature and relative humidity as well as all timing variables. The value of tailwind assistance at low altitudes (approximately 100 m) provided a better fit than tailwind assistance at higher altitudes (approximately 792 m) (see **Figure 3.15**). In **Figure 3.15**, each dot represents the number of birds detected below 200 m divided by the total number of birds observed, in each hourly bin, classified by time of night. The lines are smoothed relationships between the index, and the total number of targets on a log scale.

The primary finding expressed in **Figure 3.15** is that on nights when large numbers of targets were detected there tended to be fewer of those targets at lower altitudes.

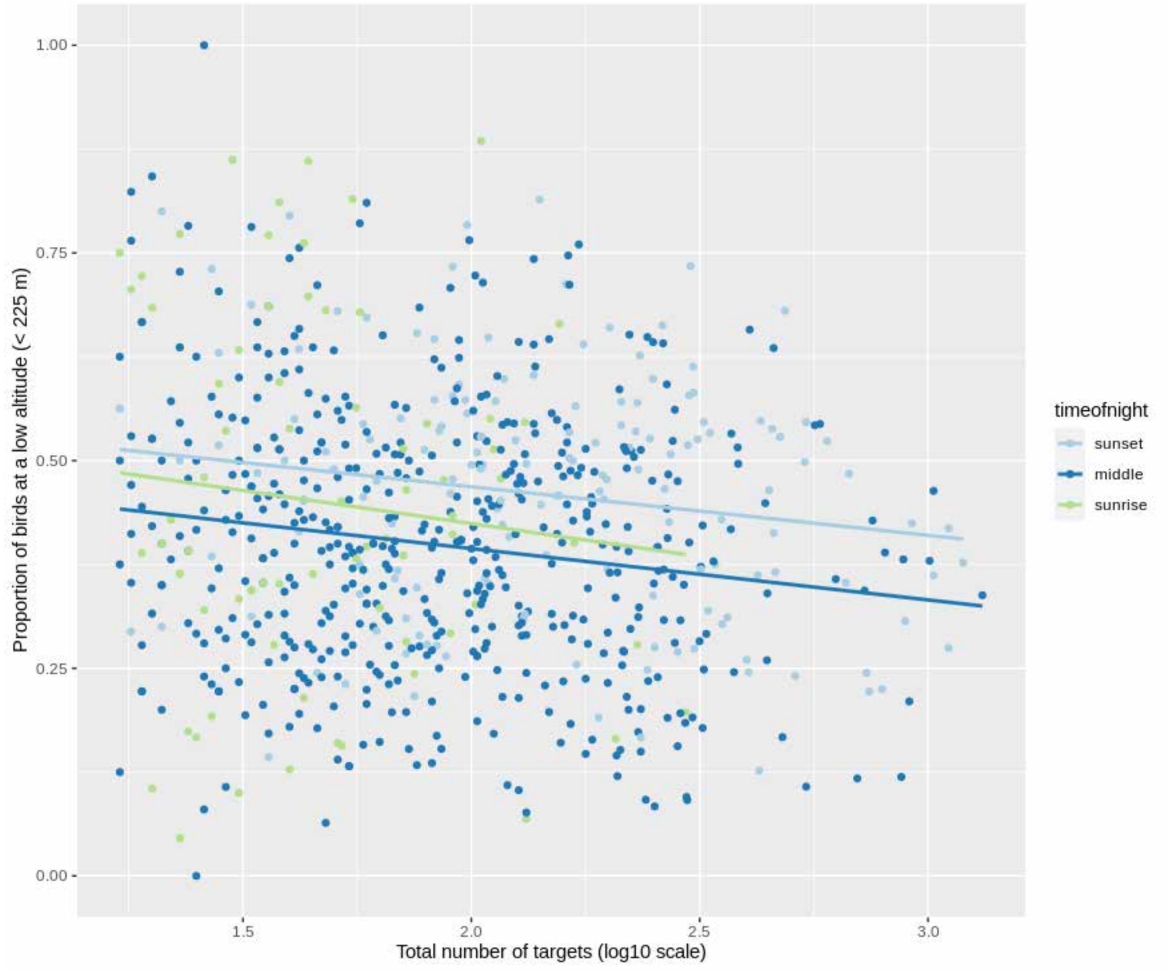

Figure 3.15 **Proportion of Targets at Low Altitude in Comparison to Total Number of Targets at Three Time Periods.**

4.0 SUMMARY

Radar and acoustic monitoring were completed at the Project area during the spring and fall 2021 migration seasons with radar data collected within approximately 1.5 km of the nearest proposed turbine and acoustic data were obtained through a network of sensors located across the Project area.

While some level of migration was observed on most nights, a large proportion of the migratory activity observed in each season was limited to a few nights. Also, most activity was observed when favourable tailwinds were present. These findings are typical to other radar and acoustic studies completed in Nova Scotia (e.g., Peckford and Taylor, 2008).

Targets were detected at heights throughout the area sampled (i.e., between 70 m and approximately 400 m in spring and approximately 800 m in the fall), with the majority being detected below 400 m. However, given that the probability of detecting small birds decreases as distance from the radar increases, the decrease in number of detections of birds higher than 400 m is likely a combination of fewer birds aloft and a decreased detectability. During the spring season, when examining nights when large numbers of targets were detected (i.e., when most of the migration occurred) there appeared to be nights when there was relatively higher densities of migration within the RSA and others when the relative density of migration was greater above the RSA. This pattern was also observed during the fall, but at a somewhat lesser extent/frequency.

The reason for the observation of migratory activity within the RSA is unclear but may be due to movements of local birds, topographical conditions at the Project area, or a function of the detection range of the radar. While local birds moving throughout the Project area may account for some of the activity observed within the RSA, because NFCs were also detected during many of these nights it is likely that the majority of these detections represent active migration. With respect to topography, it is possible that as migrants approach the general area of the Cobequid mountains they do not increase their altitude above ground level in response to the increased elevation in the general area (i.e., approximately 300 m above sea level). If the relative increased topography in the general area is the reason for migratory activity to be, at times, less than 200 m, this pattern of migration would be expected to be observed across the Cobequid region. However, this explanation is speculative given that there are no other publicly available radar or acoustic migratory data in the region, and a regional assessment of migration would likely be needed to answer the question more fully. Lastly, it should be noted that the detection limitations of the radar during the spring may give the impression that more birds are flying at lower altitudes at a select set of nights. However, it is possible that migration is occurring at higher altitudes (e.g., outside of the detection range of the radar and acoustic sensors).

When examining differences in detections within nights, most activity was observed during the early and middle of the night. Fewer detections were observed near dawn, suggesting that migrants may not be using the Project area as a stopover location (although it is possible that migrants are landing earlier in the night). However, given the consistency in distribution of activity within nights, this is less likely the reason for the activity pattern observed.

Assessment of Risk

The assessment of collision risk by migratory birds with turbines using radar and acoustic data are difficult and have not been proven to be that effective. In general, mortality associated with windfarms is thought to be low, relative to the effects of other human infrastructure (Zimmerling et al. 2013). While risk may be correlated with volume of migration, without multiple, standardized radar/acoustic studies conducted across a broader region (i.e., across Nova Scotia), it is difficult to make definitive statements about whether the volume of migrants at any particular site is more or less than what might be expected elsewhere.

Risk of migratory bird collisions is also hypothesized to be increased when birds are landing within a project area or if large numbers of birds are "forced" to fly lower due to weather variables such as fog. As indicated above, it appears from the data that large numbers of birds are not using the Project area as a stopover site. However, because during a subset of the peak nights of migration the relative density of migration was highest within the RSA, it is unclear how in-flight nocturnal migrants may interact with the Project.

5.0 CLOSURE

This work was performed in accordance with the Purchase Order between Hemmera Envirochem Inc. (Hemmera), a wholly owned subsidiary of Ausenco Engineering Canada Inc. (Ausenco), and Natural Forces Developments LP, dated March 2, 2021 (Contract). This report has been prepared by Hemmera, based on fieldwork conducted by Hemmera, for the sole benefit and use by Natural Forces Developments LP. In performing this work, Hemmera has relied in good faith on information provided by others and has assumed that the information provided by those individuals is both complete and accurate. This work was performed to current industry standard practice for similar environmental work, within the relevant jurisdiction and same locale. The findings presented herein should be considered within the context of the scope of work and Project terms of reference; further, the findings are time sensitive and are considered valid only at the time the report was produced. The conclusions and recommendations contained in this report are based upon the applicable guidelines, regulations, and legislation existing at the time the report was produced; any changes in the regulatory regime may alter the conclusions and/or recommendations.

We sincerely appreciate the opportunity to have assisted you with this Project and if there are any questions, please do not hesitate to contact the undersigned.

Report prepared by:
Hemmera Envirochem Inc.

Julie vanTol, B.Sc.
Director of Operations, Atlantic Canada
902.221.7147
jvantol@gmail.com

Report prepared by:
Hemmera Envirochem Inc.

Mike Peckford, M.Sc., P.Biol.
National Director, Power
902.488.2400
mpeckford@hemmera.com

6.0 REFERENCES

Barton, K. (2012). MuMIn: multi-model inference: R package. See: http://cran. r-project. org/web/packages. MuMIn/index. html.

Bates, D., Martin Maechler, Ben Bolker, Steve Walker (2015). Fitting Linear Mixed-Effects Models Using lme4. Journal of Statistical Software, 67(1), 1-48. DOI: 10.18637/jss.v067.i01.

Crawley, M.J. (2007). The R Book. Chichester: Wiley

Farnsworth, A. "Flight Calls and Their Value for Future Ornithological Studies and Conservation Research." 2005. The Auk 122(3): 733-746. DOI:10.1093/auk/122.3.733

Hemmera Envirochem Inc. Benjamins Mill Wind Project – Radar and Acoustic Monitoring. 2021

Kemp, M. U., Emiel van Loon, E., Shamoun-Baranes, J., Bouten, W., 2012. RNCEP: global weather and climate data at your fingertips. Methods in Ecology and Evolution (3), 65-70., DOI: 10.1111/j.2041-210X.2011.00138.x

Lightfoot, H. and P.D. Taylor. (2014). Fall radar study report – Amherst NS. URL https://novascotia.ca/nse/ea/amherst-community-wind-farm-project/Appendix-A_B.pdf

Mazerolle, M. J. (2012). Package ‘AICcmodavg’, version 1.25. R Foundation for Statistical Computing, Vienna. www. R-project. org.

Nova Scotia Government (2021). Guide to Preparing an EA Registration Document for Wind Power Projects in Nova Scotia. Environmental Assessment Branch. URL EA.Guide-Proponents-WindPowerProjects.pdf (novascotia.ca)

Peckford, M. L. (2006). Wind drift and the use of radar, acoustics, and Canadian Migration Monitoring Network methods for monitoring nocturnal passerine migration. URL https://scholar.acadiau.ca/islandora/object/theses:120

Peckford, M.L. and Taylor, P.D. (2008). Within night correlations between radar and groundcounts of migrating songbirds. J Field Ornithol. 79:207–214. DOI: 10.1111/j.1557-9263.2008.00165

R Core Team (2018). R: A language and environment for statistical computing. R Foundation for Statistical Computing, Vienna, Austria. URL https://www.R-project.org/.

Smith AD, Paton PWC, McWilliams SR (2014). Using Nocturnal Flight Calls to Assess the Fall Migration of Warblers and Sparrows along a Coastal Ecological Barrier. PLoS ONE 9(3): e92218. doi:10.1371/journal.pone.0092218

Taylor, P.D., Neima, S., and Walker, J. (2020). Burchill Energy Project Radar and Acoustic Monitoring Interim Report.

Taylor, P.D., Brzustowski, J.M., Matkovich, C. (2010). radR: an open-source platform for acquiring and analysing data on biological targets observed by surveillance radar. BMC Ecol. 10:22 . DOI: 10.1186/1472-6785-10-22

Wickham et al., (2019). Welcome to the tidyverse. Journal of Open Source Software, 4(43), 1686, DOI: 10.21105/joss.01686

Zimmerling, J., Pomeroy, A., d'Entremont, M., & Francis, C. (2013). Canadian estimate of bird mortality due to collisions and direct habitat loss associated with wind turbine developments. Avian Conservation and Ecology, 8(2).

APPENDIX A

Complete Spring and Fall Radar and Acoustic Data

OVERVIEW

The following plots provide the radar and acoustic detections and wind conditions on all nights monitoring at the Project in spring and fall 2021. Each plot is a separate night, with the beginning and end of civil twilight indicated by the vertical green and yellow lines, respectively. Date and time are on the x-axis and altitude is on the y-axis. Hexagonal points are radar detections divided into time and altitude bins and are scaled from light grey (few detections) through dark purple to yellow (many detections). Acoustic detections (a single NFC) are red points along the base of each plot (These have not been processed, and so on some nights may be contaminated by insects, raindrops or other noise). Wind direction and strength at the surface (red arrow) and aloft (790 m; green arrow) for each hour are displayed at the top of each plot. The blue box represents a period of rain when we were unable to distinguish between raindrops and bird detections. Red lines represent the approximate altitudinal range of the rotor sweep area.

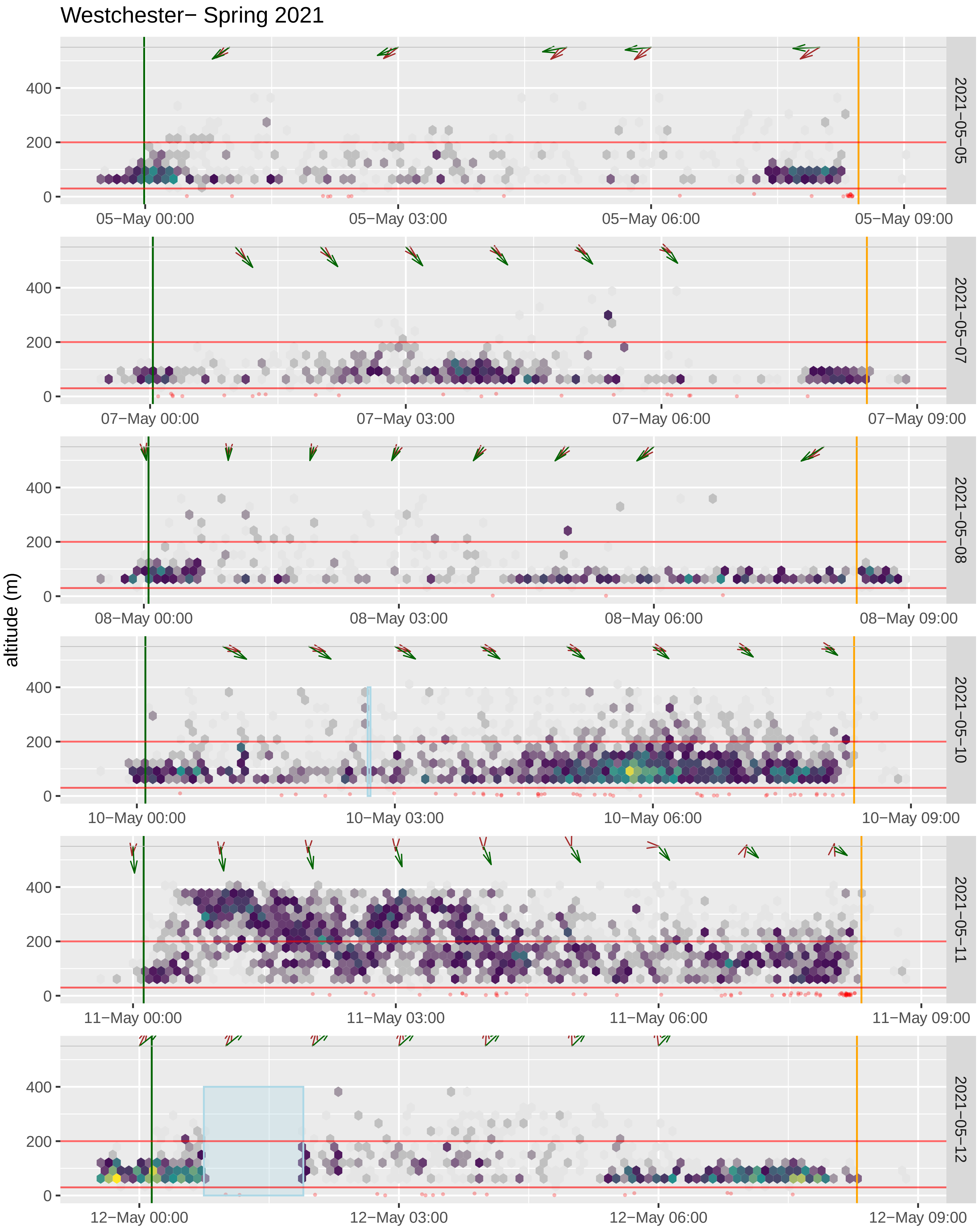
Westchester− Spring 2021
altitude (m)
400
200
0
05−May 00:00
05−May 03:00
05−May 06:00
05−May 09:00
2021−05−05
07−May 00:00
07−May 03:00
07−May 06:00
07−May 09:00
2021−05−07
08−May 00:00
08−May 03:00
08−May 06:00
08−May 09:00
2021−05−08
10−May 00:00
10−May 03:00
10−May 06:00
10−May 09:00
2021−05−10
11−May 00:00
11−May 03:00
11−May 06:00
11−May 09:00
2021−05−11
12−May 00:00
12−May 03:00
12−May 06:00
12−May 09:00
2021−05−12

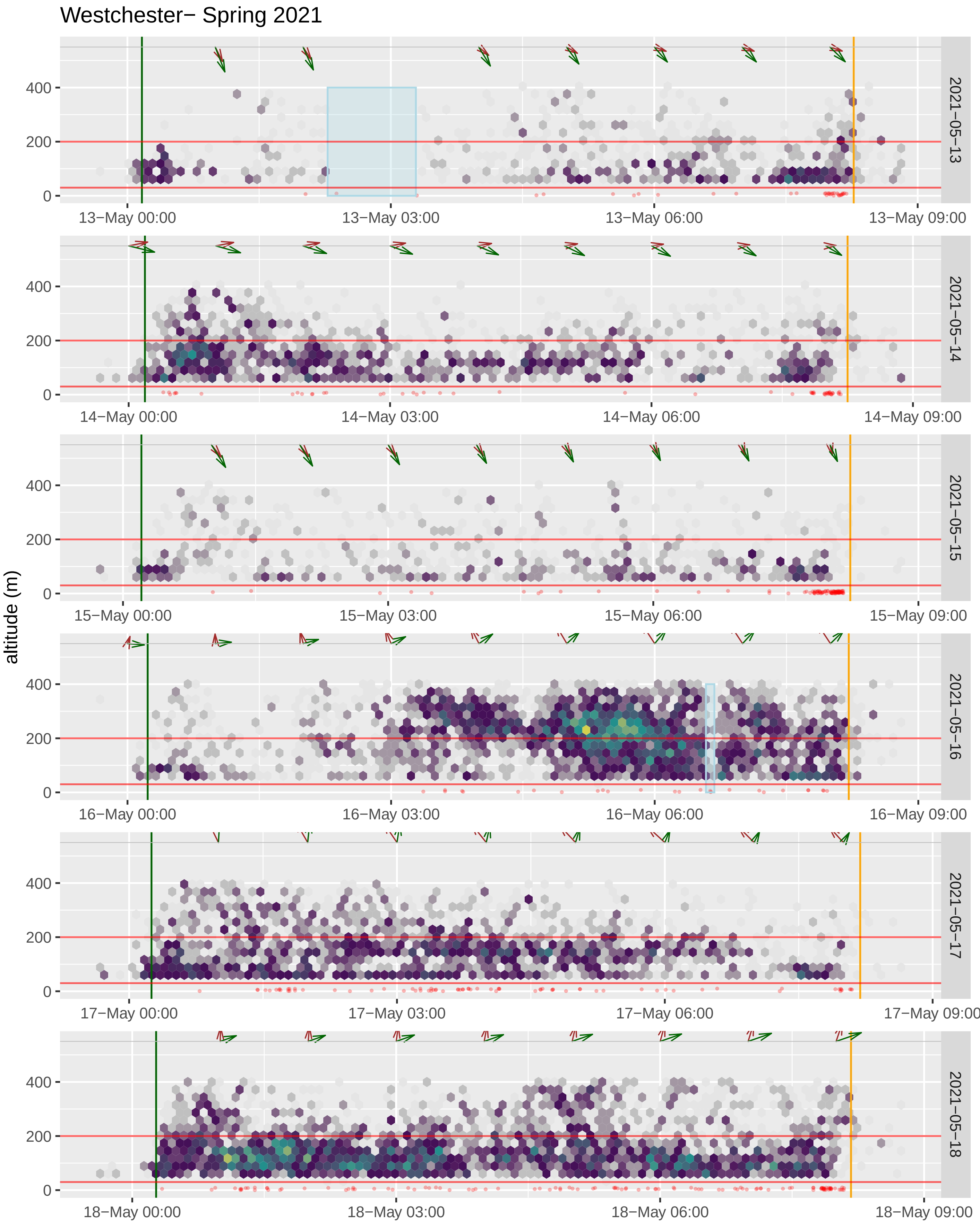
Westchester− Spring 2021
altitude (m)
0
200
400
13−May 00:00
13−May 03:00
13−May 06:00
13−May 09:00
2021−05−13
14−May 00:00
14−May 03:00
14−May 06:00
14−May 09:00
2021−05−14
15−May 00:00
15−May 03:00
15−May 06:00
15−May 09:00
2021−05−15
16−May 00:00
16−May 03:00
16−May 06:00
16−May 09:00
2021−05−16
17−May 00:00
17−May 03:00
17−May 06:00
17−May 09:00
2021−05−17
18−May 00:00
18−May 03:00
18−May 06:00
18−May 09:00
2021−05−18

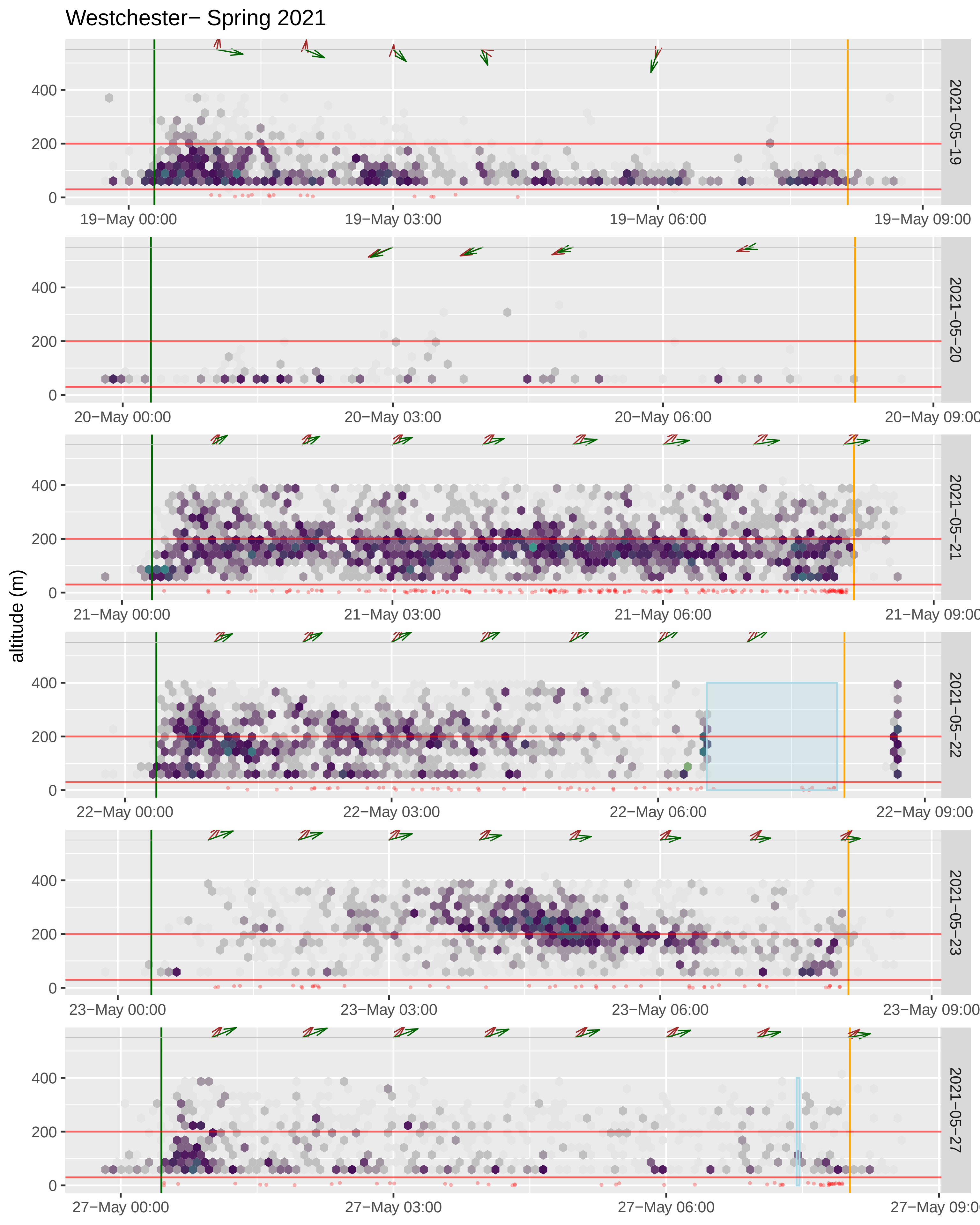
Westchester− Spring 2021
altitude (m)
400
200
0
19−May 00:00
19−May 03:00
19−May 06:00
19−May 09:00
2021−05−19
20−May 00:00
20−May 03:00
20−May 06:00
20−May 09:00
2021−05−20
21−May 00:00
21−May 03:00
21−May 06:00
21−May 09:00
2021−05−21
22−May 00:00
22−May 03:00
22−May 06:00
22−May 09:00
2021−05−22
23−May 00:00
23−May 03:00
23−May 06:00
23−May 09:00
2021−05−23
27−May 00:00
27−May 03:00
27−May 06:00
27−May 09:00
2021−05−27

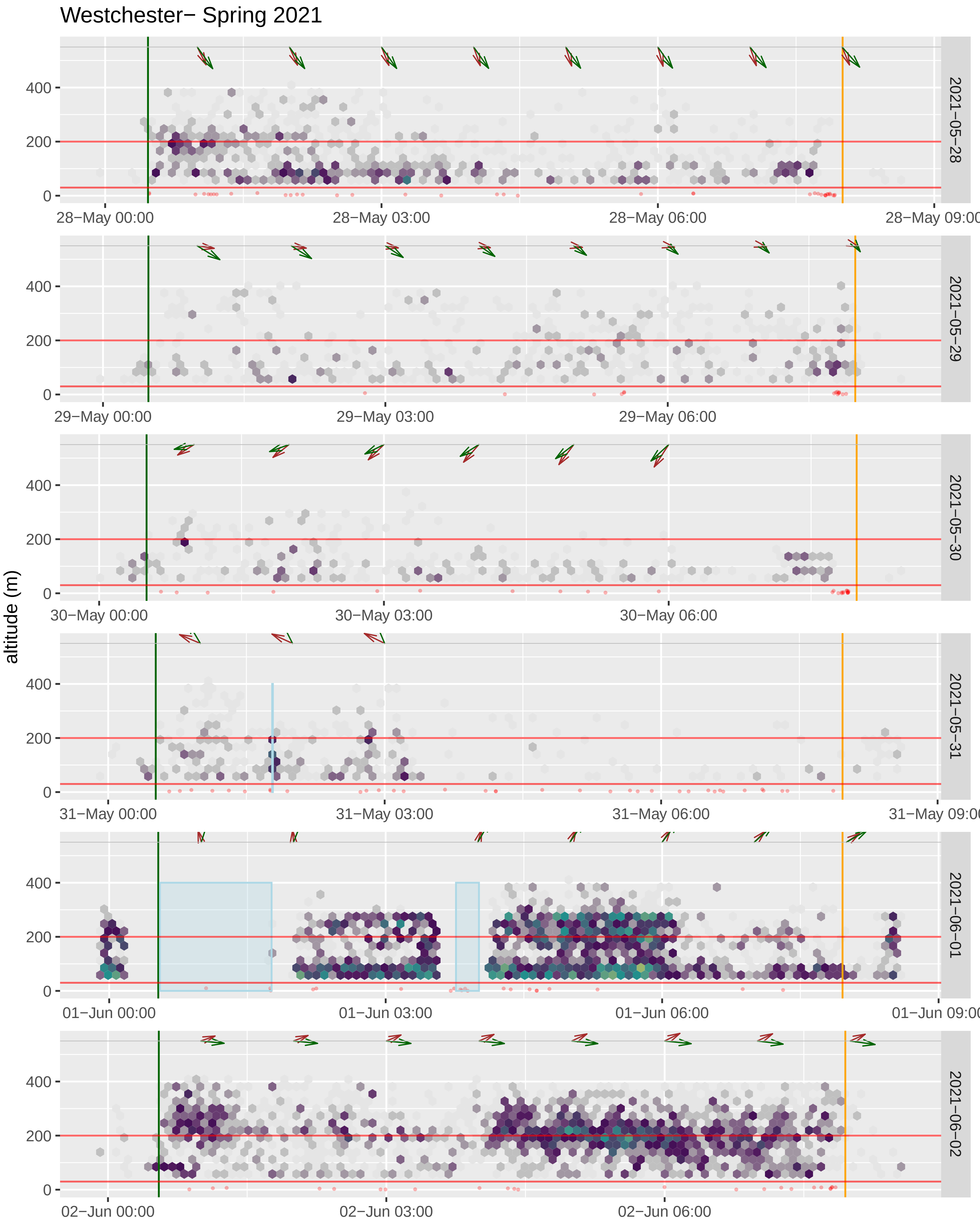
Westchester− Spring 2021
altitude (m)
400
200
0
28−May 00:00
28−May 03:00
28−May 06:00
28−May 09:00
2021−05−28
29−May 00:00
29−May 03:00
29−May 06:00
2021−05−29
30−May 00:00
30−May 03:00
30−May 06:00
2021−05−30
31−May 00:00
31−May 03:00
31−May 06:00
31−May 09:00
2021−05−31
01−Jun 00:00
01−Jun 03:00
01−Jun 06:00
01−Jun 09:00
2021−06−01
02−Jun 00:00
02−Jun 03:00
02−Jun 06:00
2021−06−02

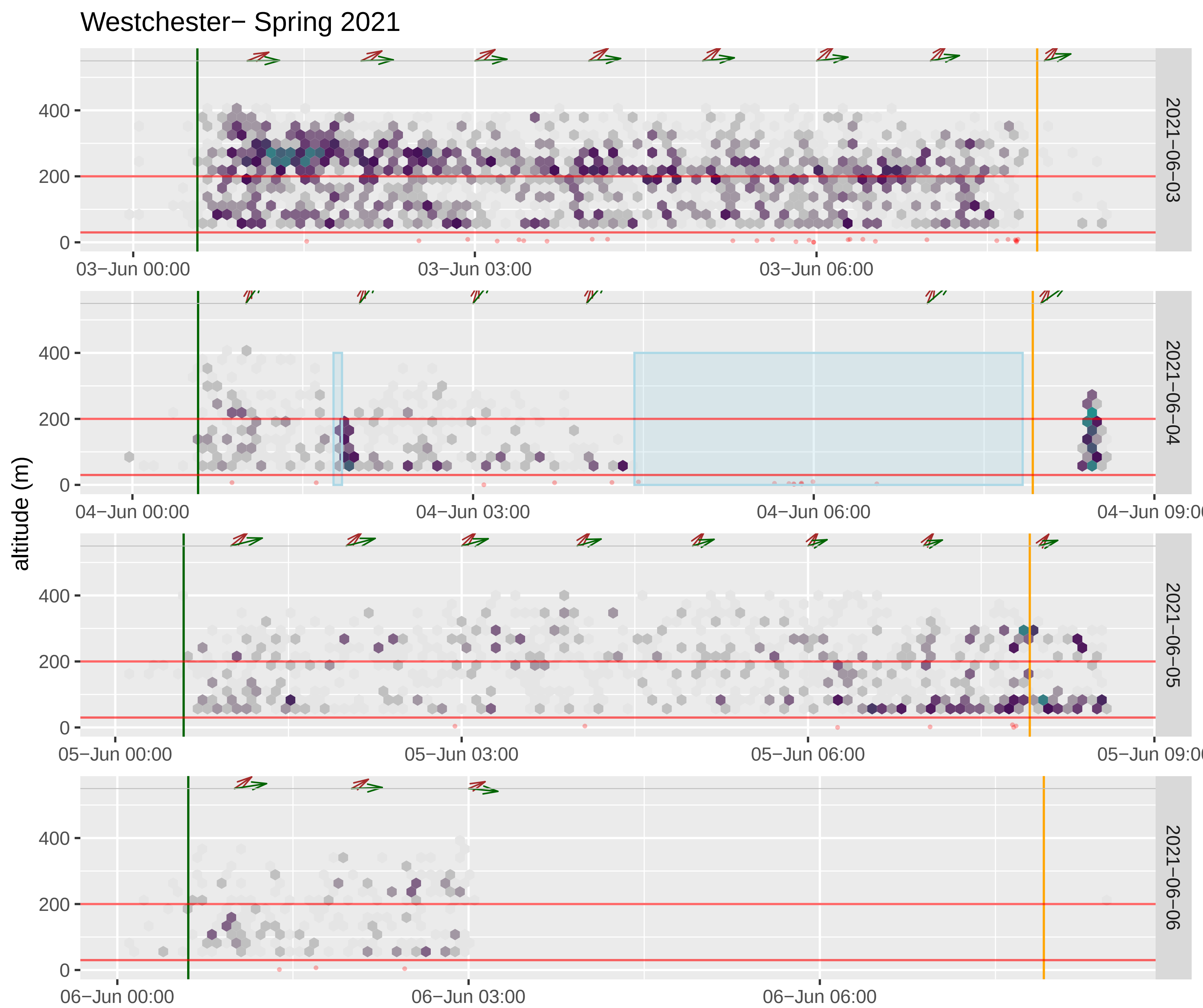
Westchester− Spring 2021
altitude (m)
400
200
0
03−Jun 00:00
03−Jun 03:00
03−Jun 06:00
2021−06−03
04−Jun 00:00
04−Jun 03:00
04−Jun 06:00
04−Jun 09:00
2021−06−04
05−Jun 00:00
05−Jun 03:00
05−Jun 06:00
05−Jun 09:00
2021−06−05
06−Jun 00:00
06−Jun 03:00
06−Jun 06:00
2021−06−06

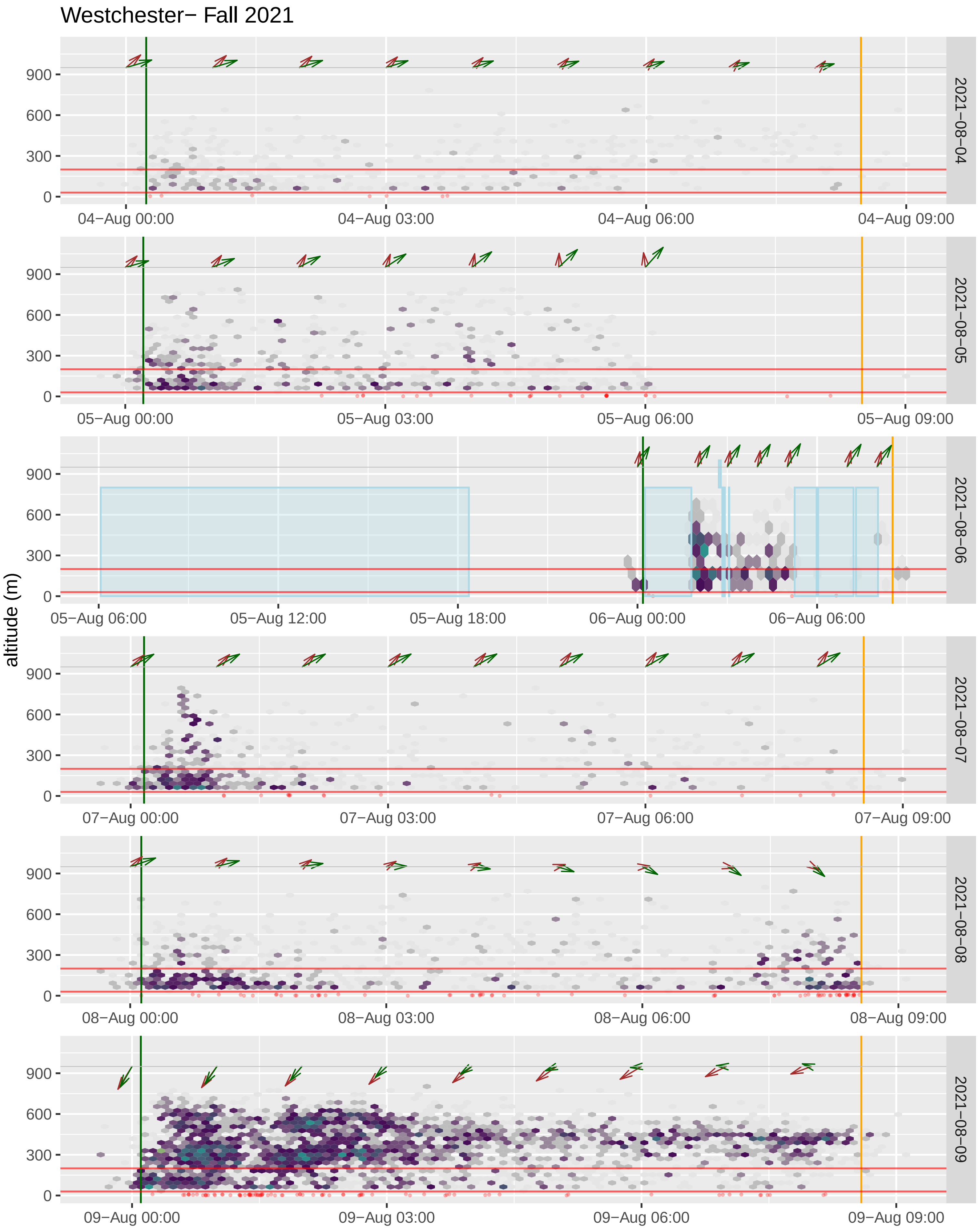
Westchester− Fall 2021
altitude (m)
900
600
300
0
04−Aug 00:00
04−Aug 03:00
04−Aug 06:00
04−Aug 09:00
2021−08−04
05−Aug 00:00
05−Aug 03:00
05−Aug 06:00
05−Aug 09:00
2021−08−05
05−Aug 06:00
05−Aug 12:00
05−Aug 18:00
06−Aug 00:00
06−Aug 06:00
2021−08−06
07−Aug 00:00
07−Aug 03:00
07−Aug 06:00
07−Aug 09:00
2021−08−07
08−Aug 00:00
08−Aug 03:00
08−Aug 06:00
08−Aug 09:00
2021−08−08
09−Aug 00:00
09−Aug 03:00
09−Aug 06:00
09−Aug 09:00
2021−08−09

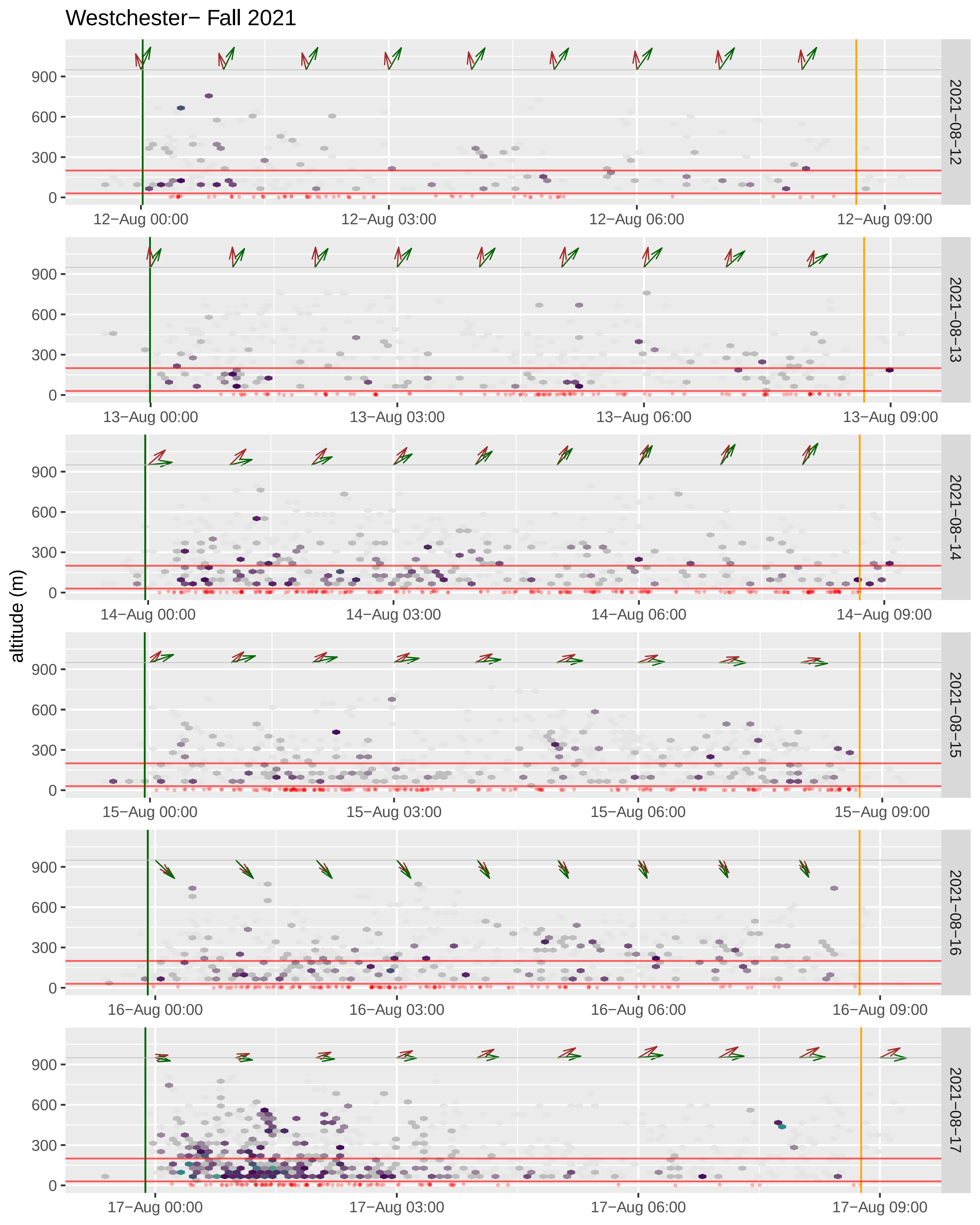
Westchester− Fall 2021
altitude (m)
0
300
600
900
12−Aug 00:00
12−Aug 03:00
12−Aug 06:00
12−Aug 09:00
2021−08−12
13−Aug 00:00
13−Aug 03:00
13−Aug 06:00
13−Aug 09:00
2021−08−13
14−Aug 00:00
14−Aug 03:00
14−Aug 06:00
14−Aug 09:00
2021−08−14
15−Aug 00:00
15−Aug 03:00
15−Aug 06:00
15−Aug 09:00
2021−08−15
16−Aug 00:00
16−Aug 03:00
16−Aug 06:00
16−Aug 09:00
2021−08−16
17−Aug 00:00
17−Aug 03:00
17−Aug 06:00
17−Aug 09:00
2021−08−17

Westchester− Fall 2021

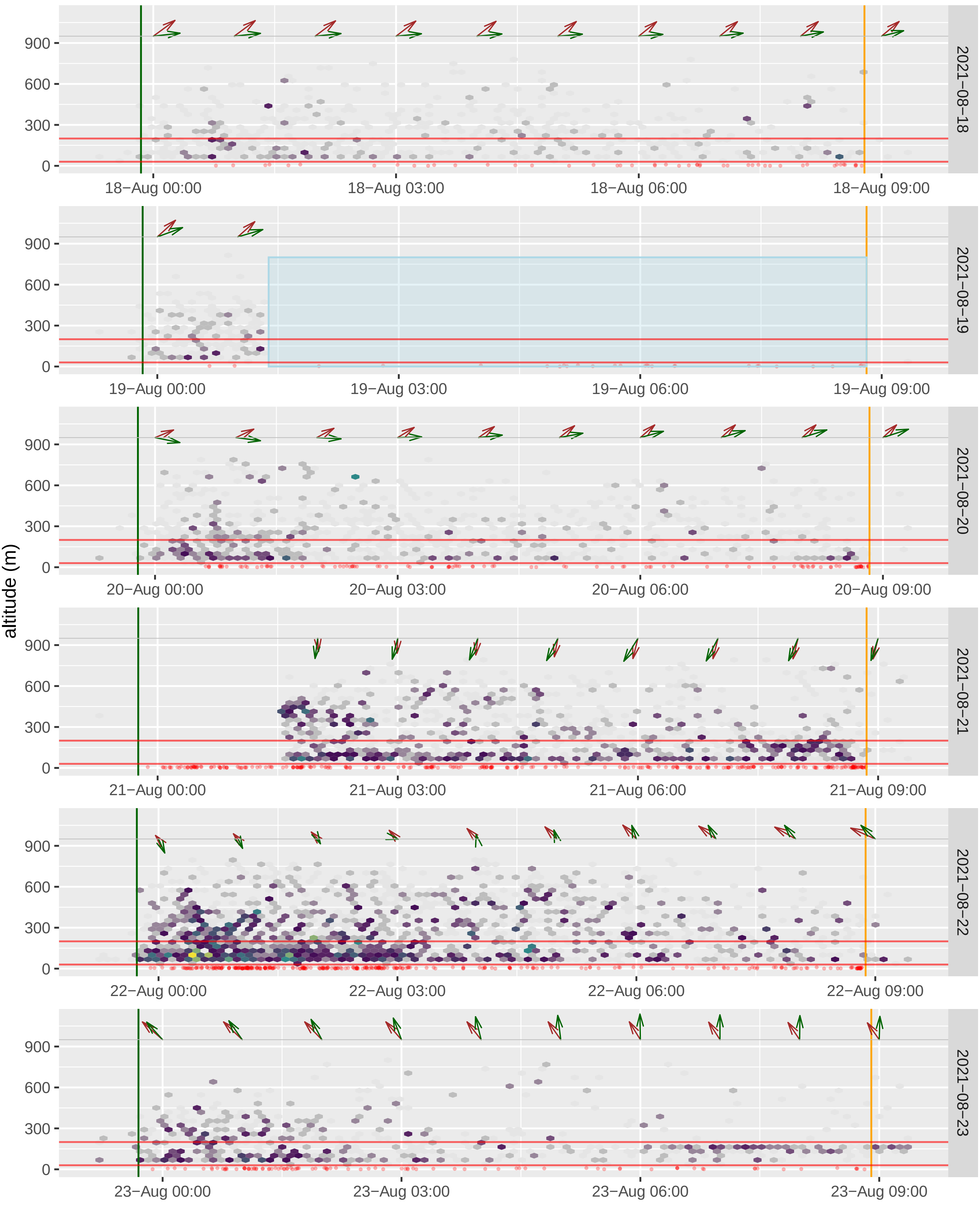

Westchester− Fall 2021

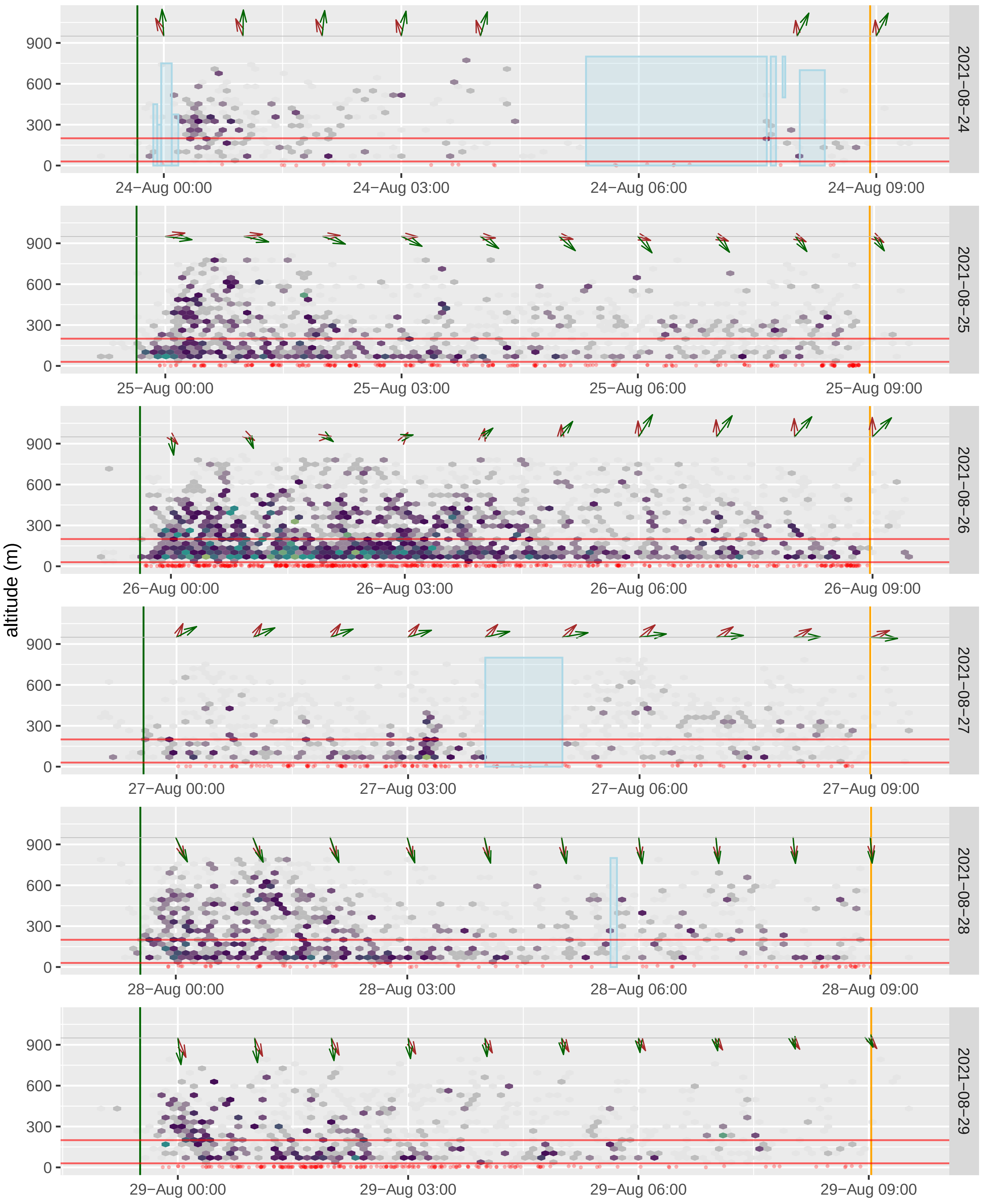

Westchester− Fall 2021

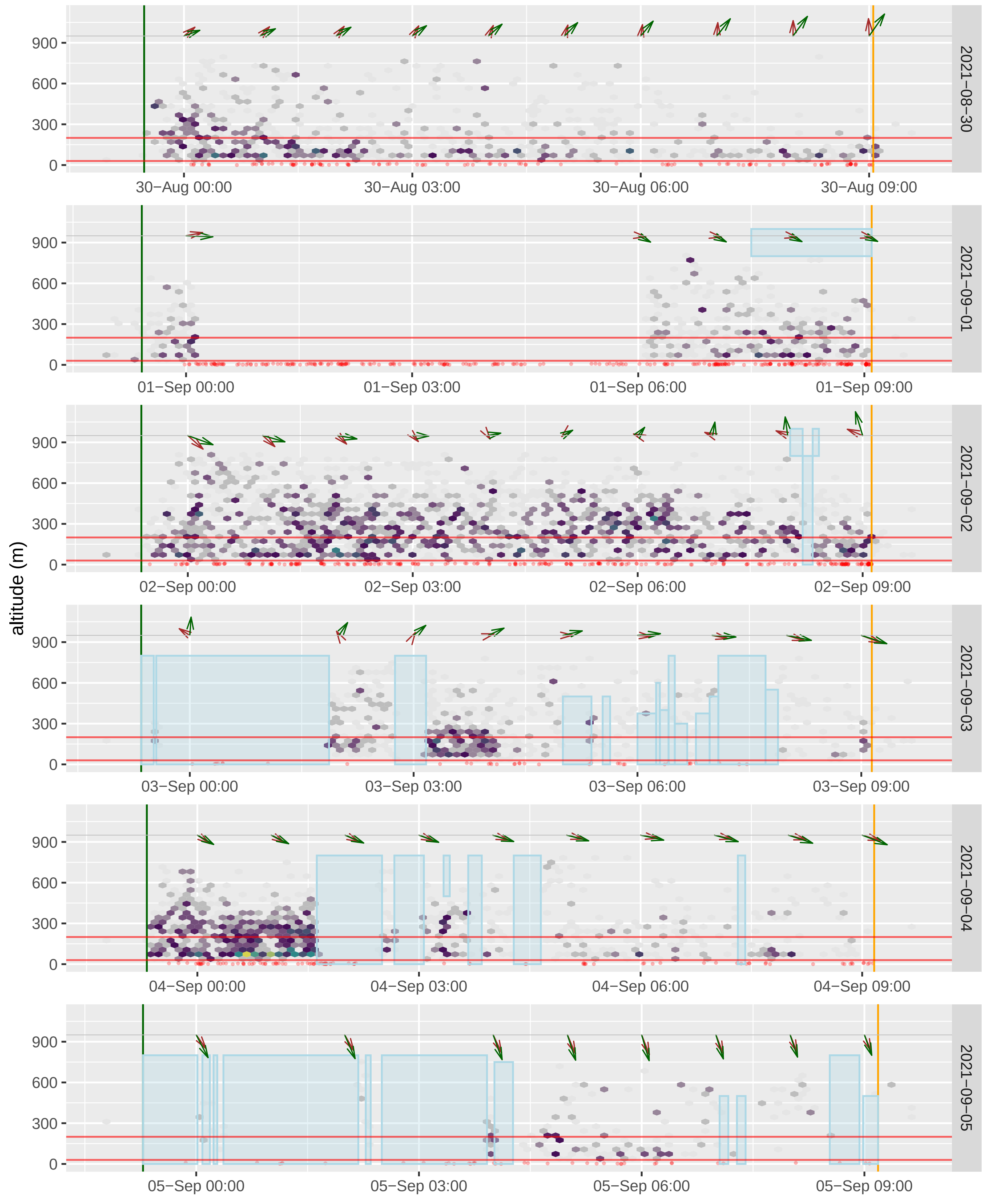

Westchester− Fall 2021

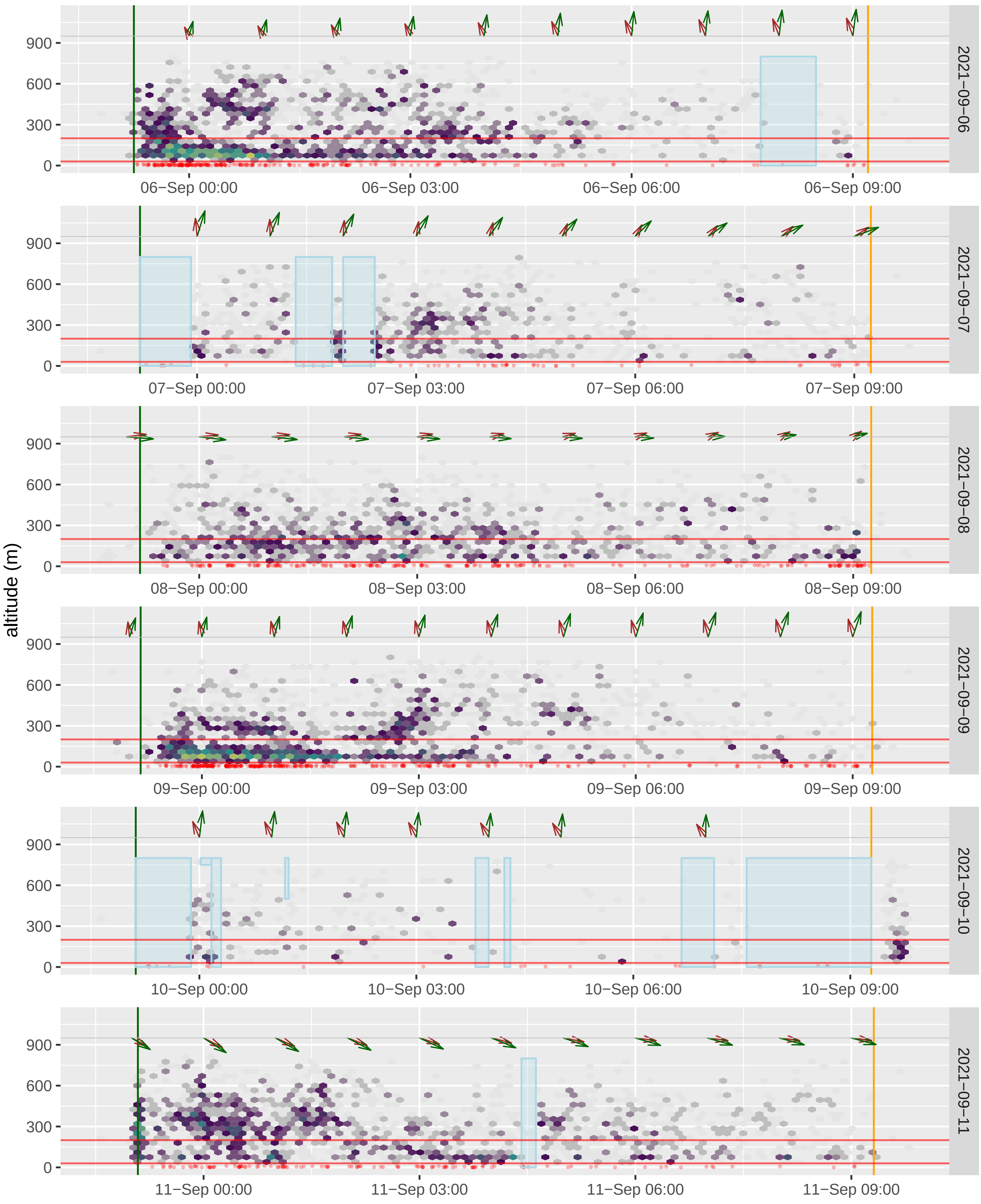

Westchester− Fall 2021

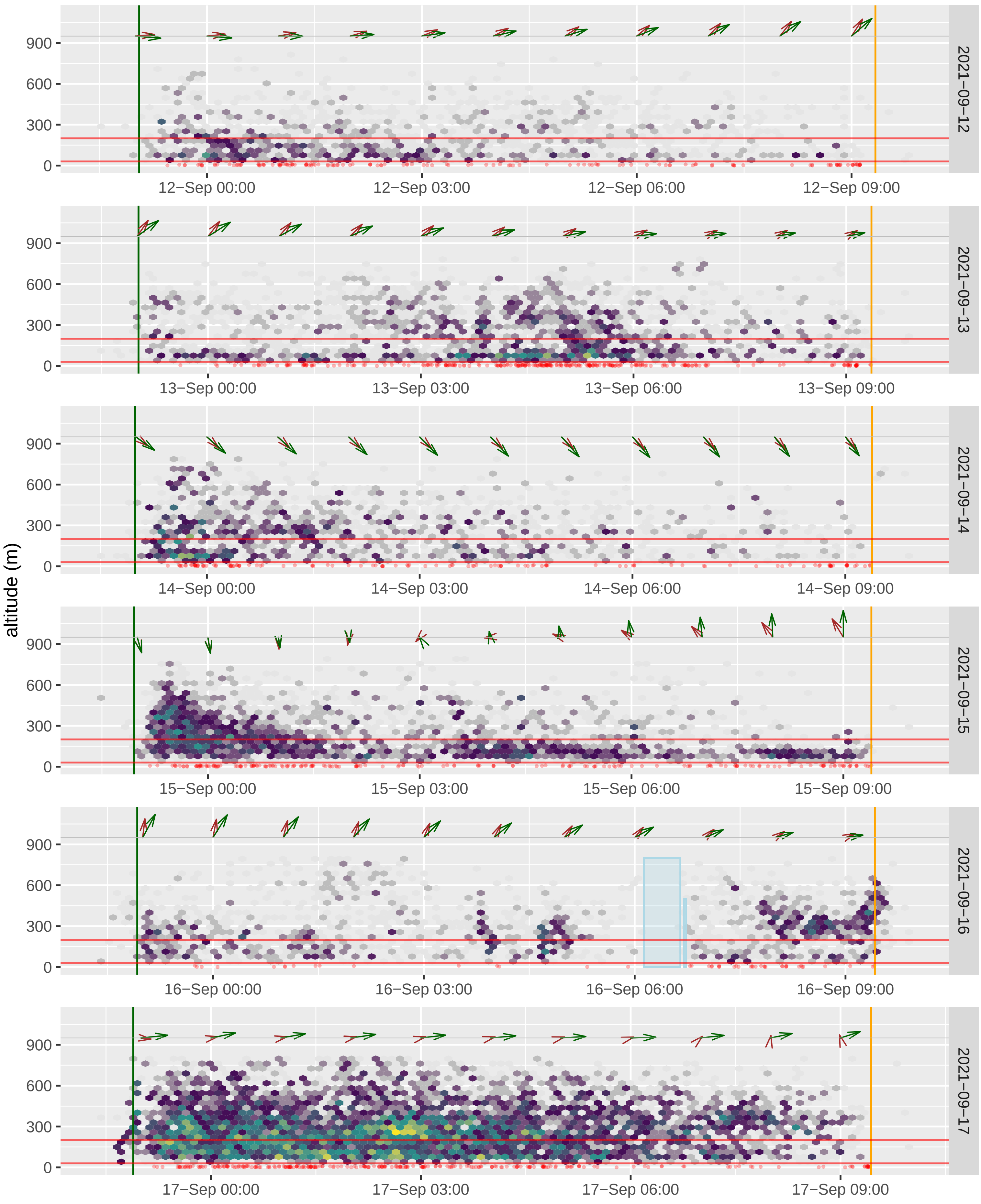

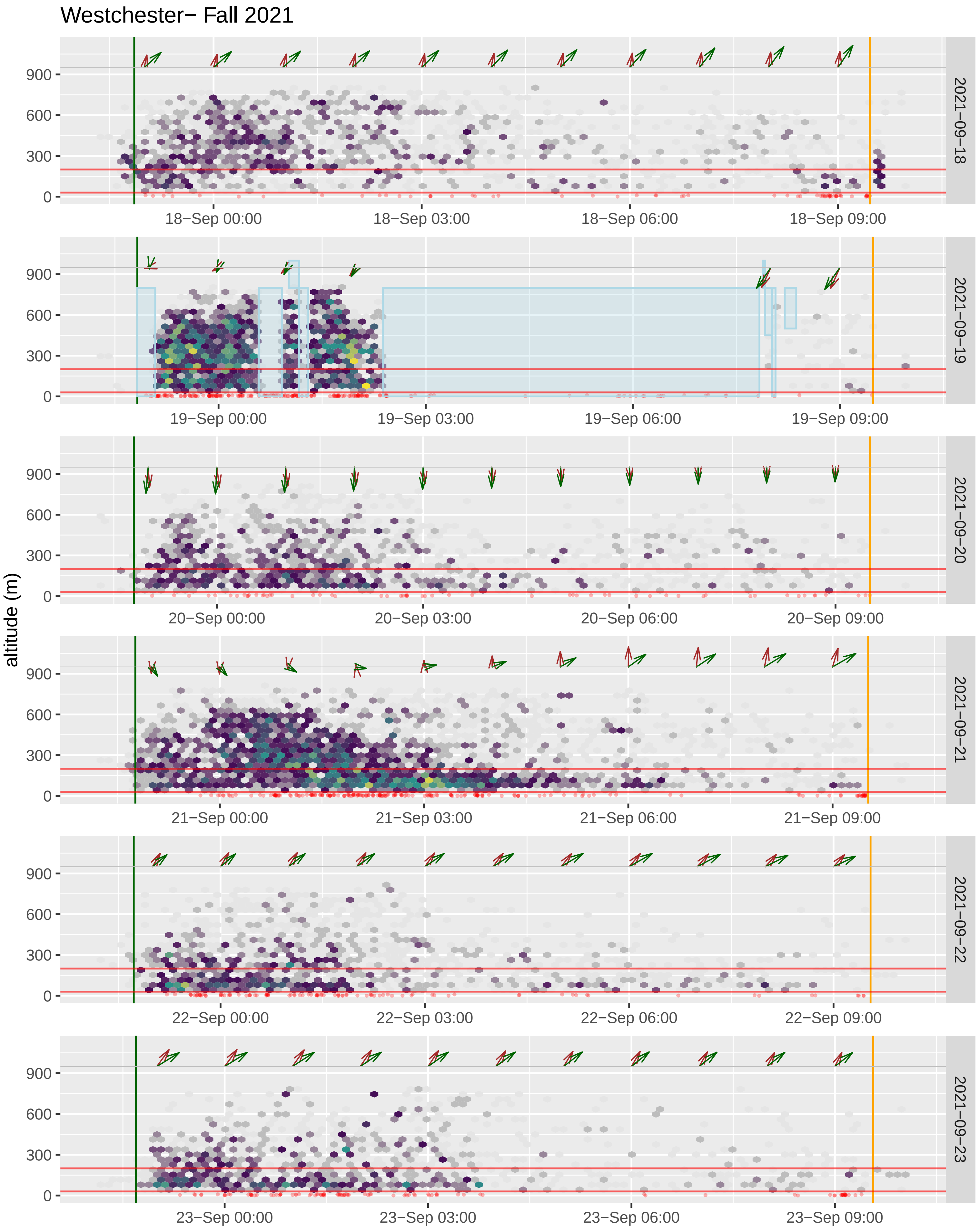
Westchester− Fall 2021
altitude (m)
0
300
600
900
18−Sep 00:00
18−Sep 03:00
18−Sep 06:00
18−Sep 09:00
2021−09−18
19−Sep 00:00
19−Sep 03:00
19−Sep 06:00
19−Sep 09:00
2021−09−19
20−Sep 00:00
20−Sep 03:00
20−Sep 06:00
20−Sep 09:00
2021−09−20
21−Sep 00:00
21−Sep 03:00
21−Sep 06:00
21−Sep 09:00
2021−09−21
22−Sep 00:00
22−Sep 03:00
22−Sep 06:00
22−Sep 09:00
2021−09−22
23−Sep 00:00
23−Sep 03:00
23−Sep 06:00
23−Sep 09:00
2021−09−23

Westchester− Fall 2021

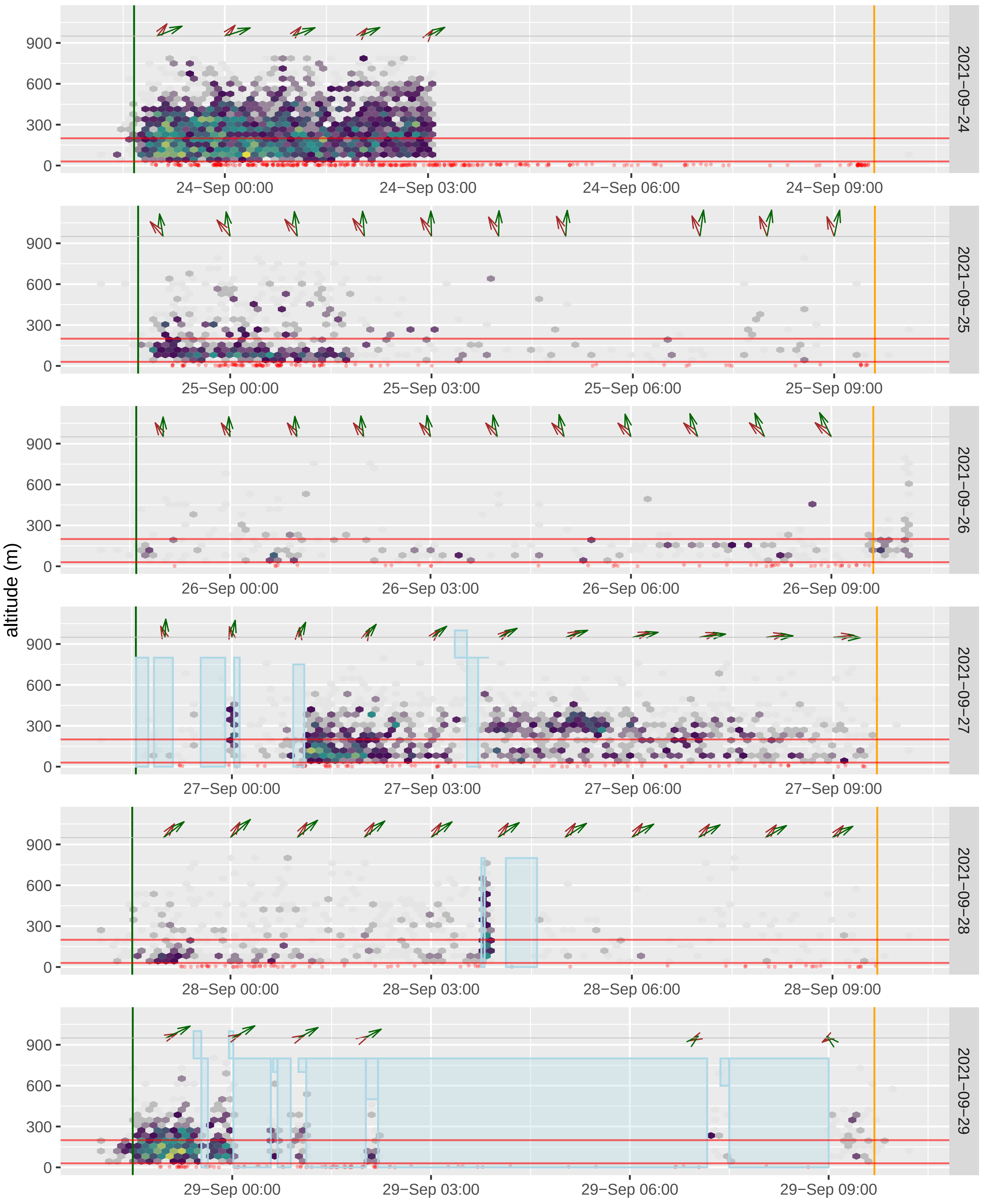

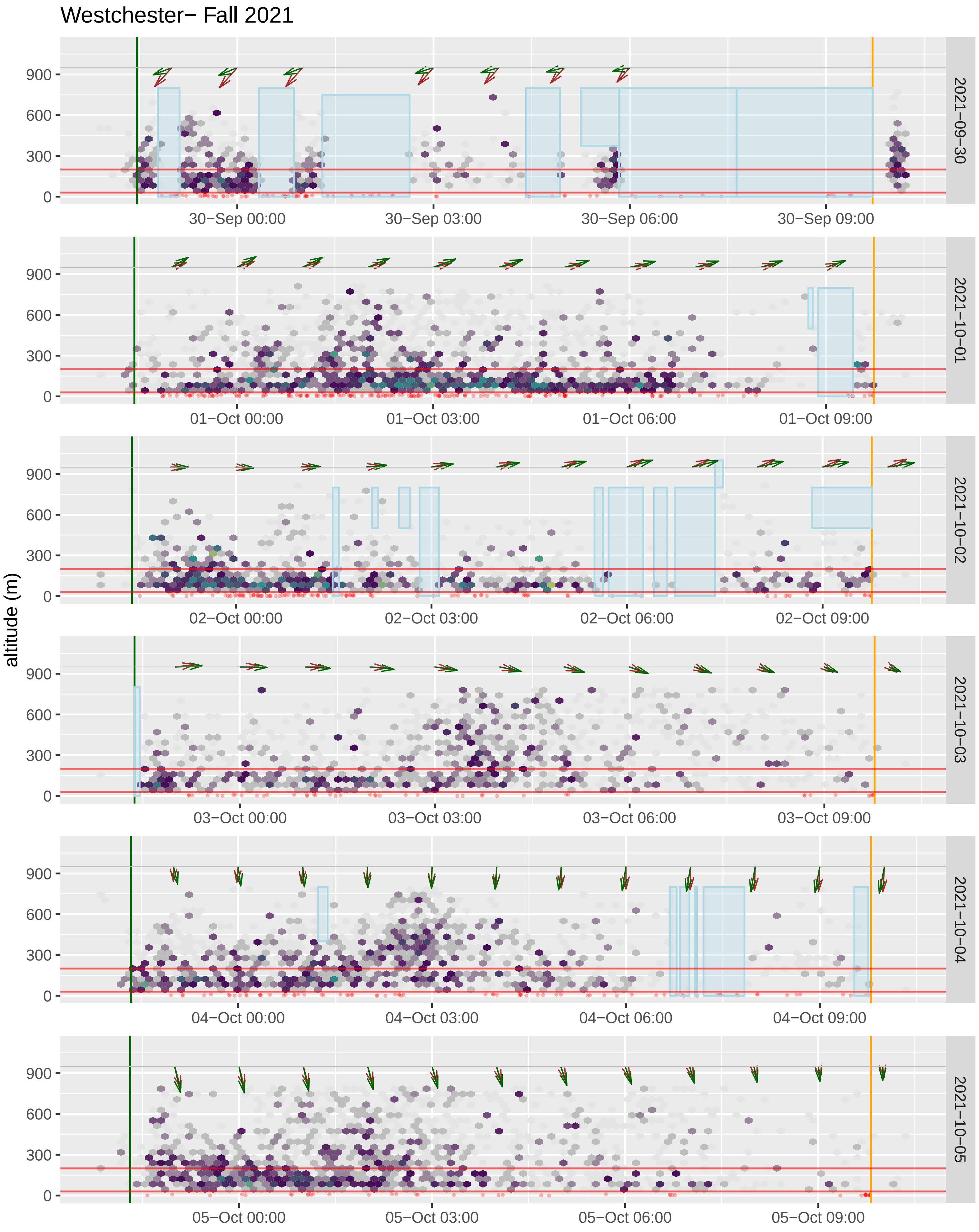
Westchester− Fall 2021
altitude (m)
0
300
600
900
30−Sep 00:00
30−Sep 03:00
30−Sep 06:00
30−Sep 09:00
2021−09−30
01−Oct 00:00
01−Oct 03:00
01−Oct 06:00
01−Oct 09:00
2021−10−01
02−Oct 00:00
02−Oct 03:00
02−Oct 06:00
02−Oct 09:00
2021−10−02
03−Oct 00:00
03−Oct 03:00
03−Oct 06:00
03−Oct 09:00
2021−10−03
04−Oct 00:00
04−Oct 03:00
04−Oct 06:00
04−Oct 09:00
2021−10−04
05−Oct 00:00
05−Oct 03:00
05−Oct 06:00
05−Oct 09:00
2021−10−05

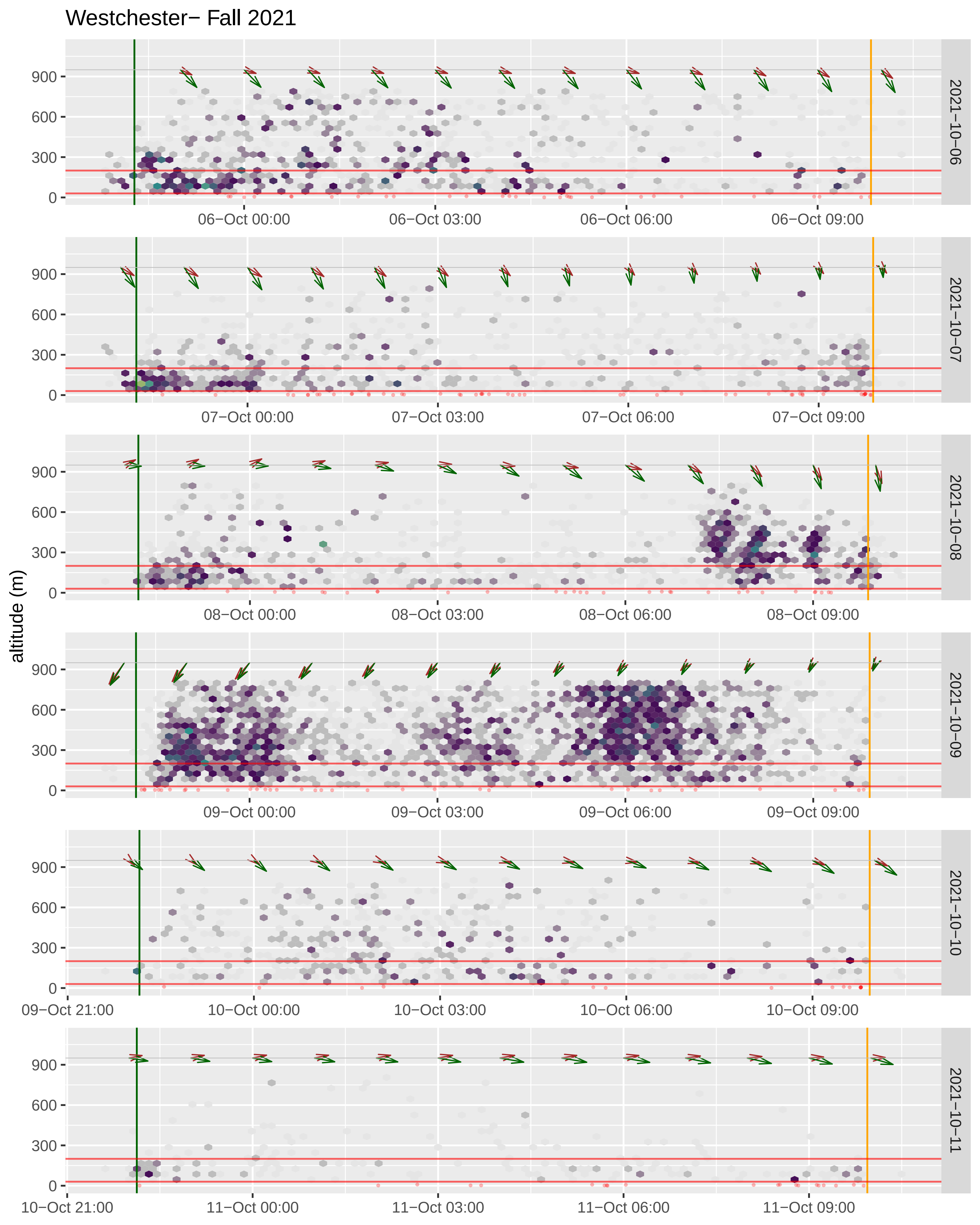
Westchester− Fall 2021
altitude (m)
900
600
300
0
06−Oct 00:00
06−Oct 03:00
06−Oct 06:00
06−Oct 09:00
2021−10−06
07−Oct 00:00
07−Oct 03:00
07−Oct 06:00
07−Oct 09:00
2021−10−07
08−Oct 00:00
08−Oct 03:00
08−Oct 06:00
08−Oct 09:00
2021−10−08
09−Oct 00:00
09−Oct 03:00
09−Oct 06:00
09−Oct 09:00
2021−10−09
09−Oct 21:00
10−Oct 00:00
10−Oct 03:00
10−Oct 06:00
10−Oct 09:00
2021−10−10
10−Oct 21:00
11−Oct 00:00
11−Oct 03:00
11−Oct 06:00
11−Oct 09:00
2021−10−11

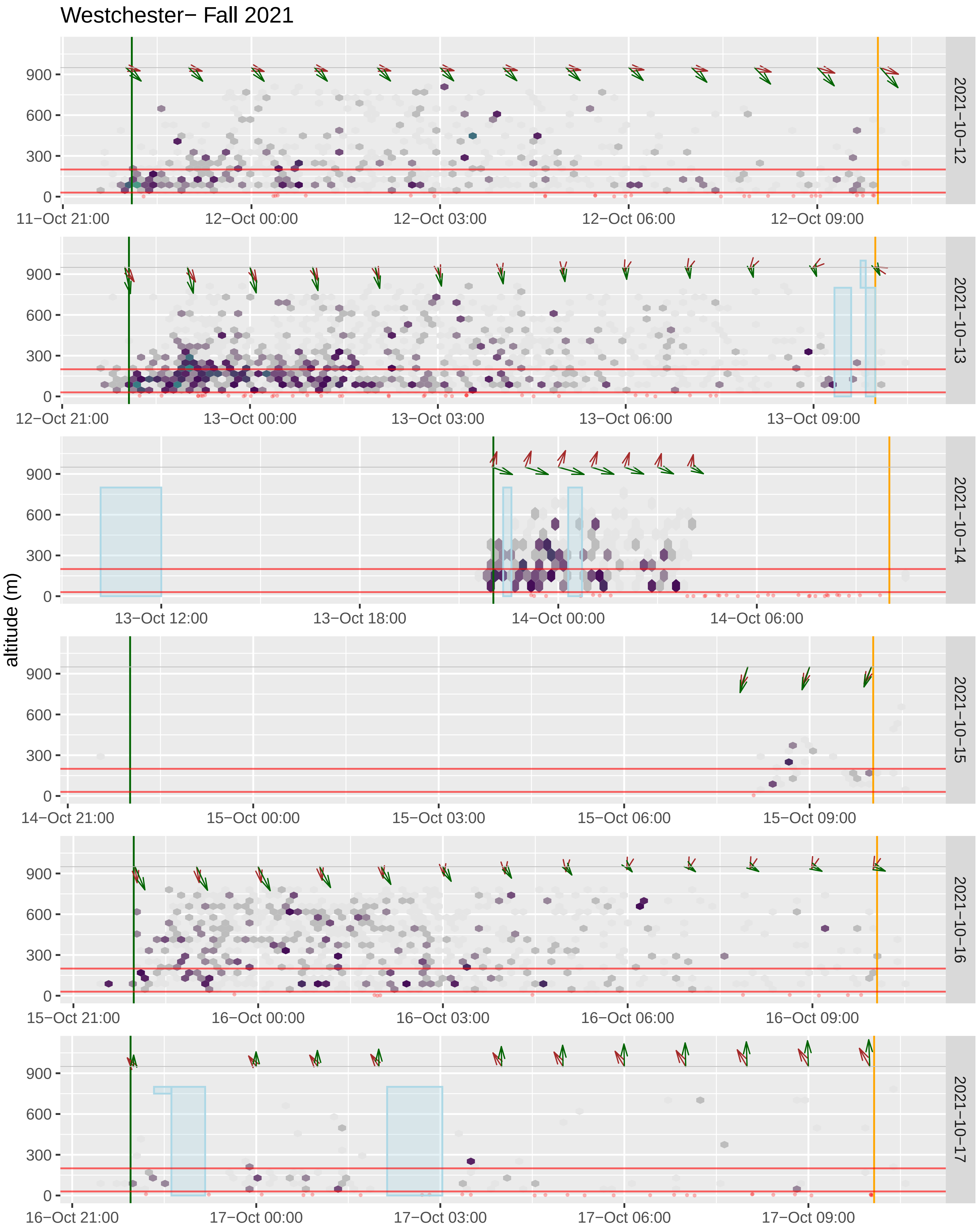
Westchester– Fall 2021
altitude (m)
900
600
300
0
11–Oct 21:00
12–Oct 00:00
12–Oct 03:00
12–Oct 06:00
12–Oct 09:00
2021–10–12
12–Oct 21:00
13–Oct 00:00
13–Oct 03:00
13–Oct 06:00
13–Oct 09:00
2021–10–13
13–Oct 12:00
13–Oct 18:00
14–Oct 00:00
14–Oct 06:00
2021–10–14
14–Oct 21:00
15–Oct 00:00
15–Oct 03:00
15–Oct 06:00
15–Oct 09:00
2021–10–15
15–Oct 21:00
16–Oct 00:00
16–Oct 03:00
16–Oct 06:00
16–Oct 09:00
2021–10–16
16–Oct 21:00
17–Oct 00:00
17–Oct 03:00
17–Oct 06:00
17–Oct 09:00
2021–10–17

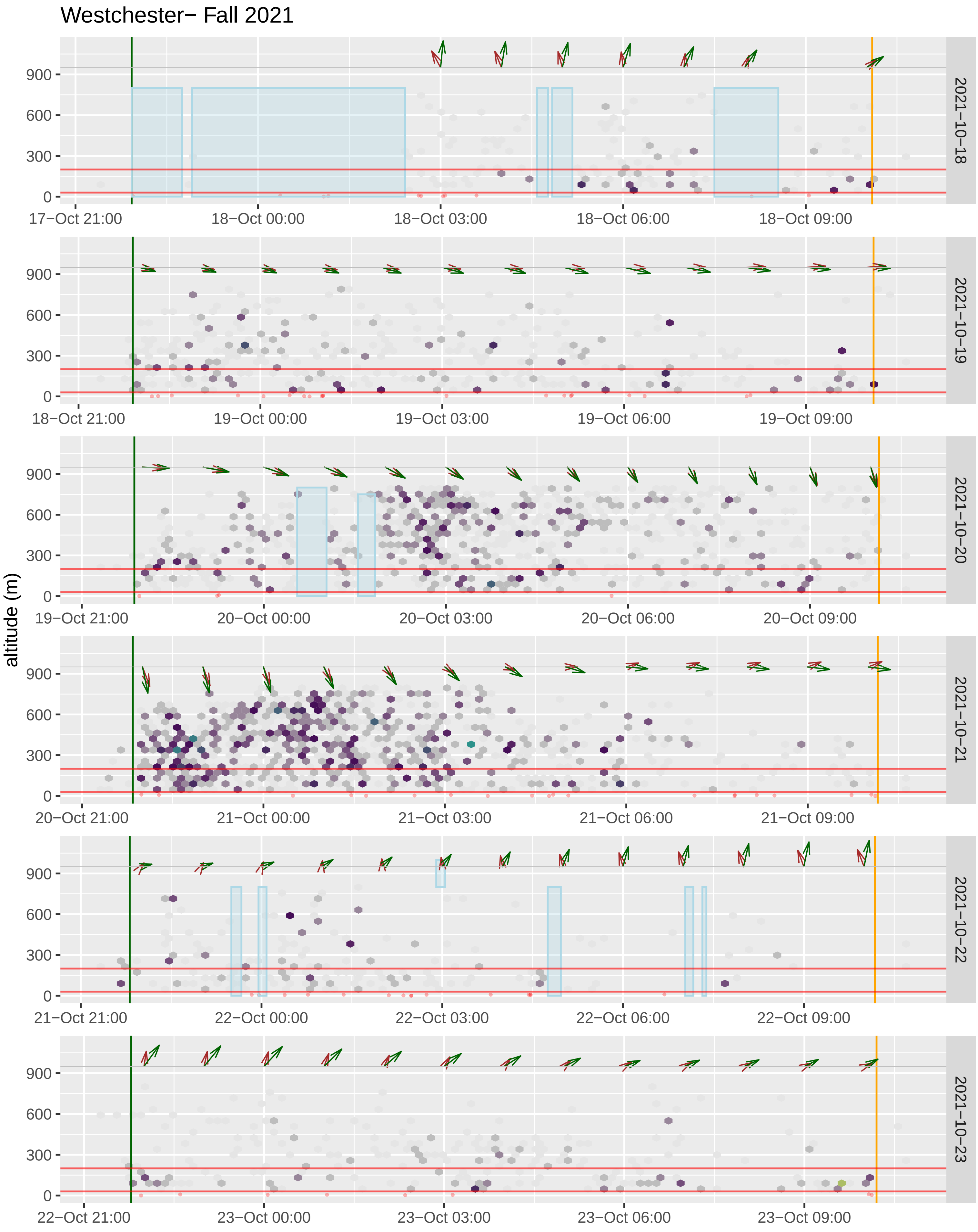
Westchester– Fall 2021
altitude (m)
900
600
300
0
17–Oct 21:00
18–Oct 00:00
18–Oct 03:00
18–Oct 06:00
18–Oct 09:00
2021–10–18
18–Oct 21:00
19–Oct 00:00
19–Oct 03:00
19–Oct 06:00
19–Oct 09:00
2021–10–19
19–Oct 21:00
20–Oct 00:00
20–Oct 03:00
20–Oct 06:00
20–Oct 09:00
2021–10–20
20–Oct 21:00
21–Oct 00:00
21–Oct 03:00
21–Oct 06:00
21–Oct 09:00
2021–10–21
21–Oct 21:00
22–Oct 00:00
22–Oct 03:00
22–Oct 06:00
22–Oct 09:00
2021–10–22
22–Oct 21:00
23–Oct 00:00
23–Oct 03:00
23–Oct 06:00
23–Oct 09:00
2021–10–23

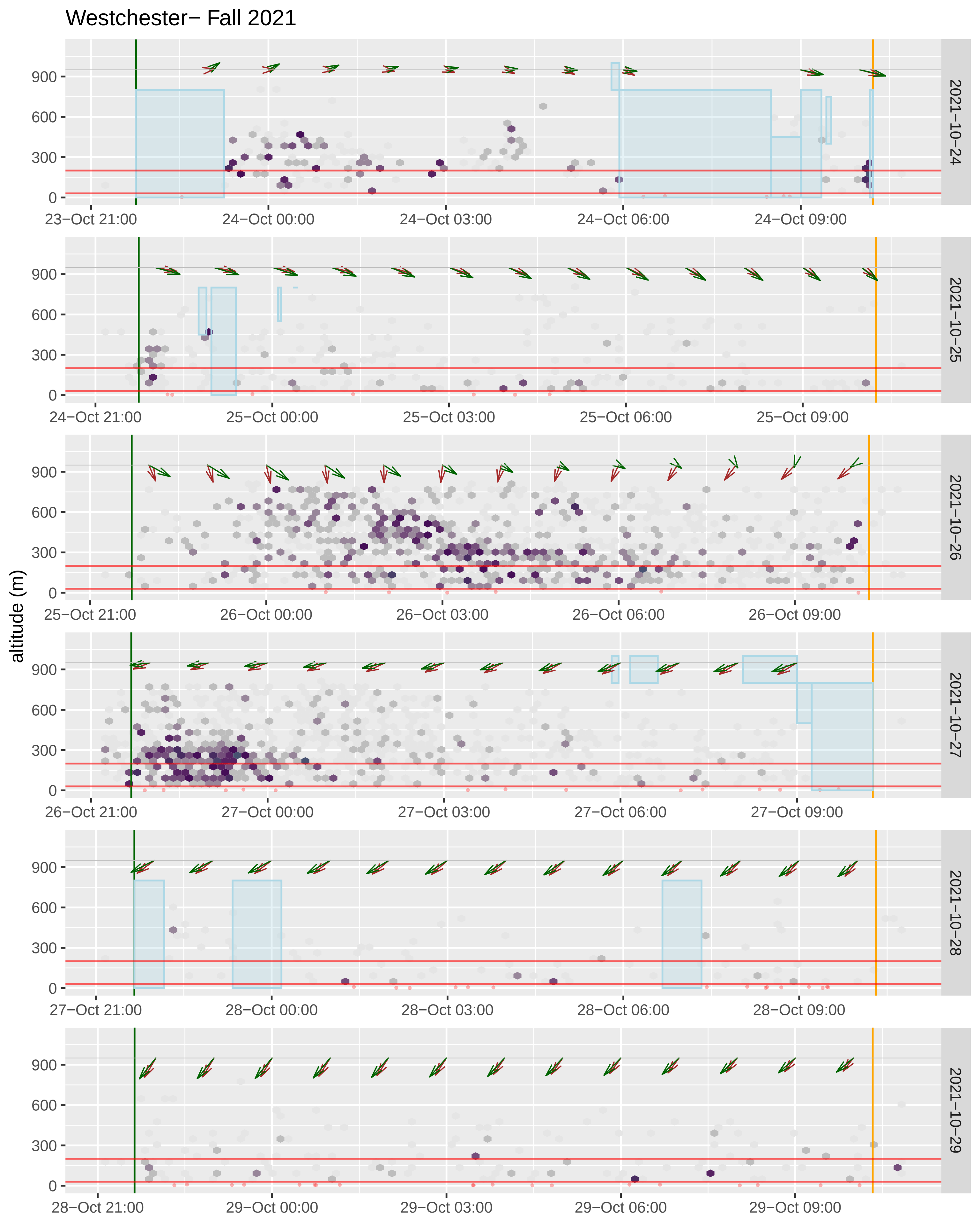
Westchester− Fall 2021
altitude (m)
900
600
300
0
23−Oct 21:00
24−Oct 00:00
24−Oct 03:00
24−Oct 06:00
24−Oct 09:00
2021−10−24
24−Oct 21:00
25−Oct 00:00
25−Oct 03:00
25−Oct 06:00
25−Oct 09:00
2021−10−25
25−Oct 21:00
26−Oct 00:00
26−Oct 03:00
26−Oct 06:00
26−Oct 09:00
2021−10−26
26−Oct 21:00
27−Oct 00:00
27−Oct 03:00
27−Oct 06:00
27−Oct 09:00
2021−10−27
27−Oct 21:00
28−Oct 00:00
28−Oct 03:00
28−Oct 06:00
28−Oct 09:00
2021−10−28
28−Oct 21:00
29−Oct 00:00
29−Oct 03:00
29−Oct 06:00
29−Oct 09:00
2021−10−29

Westchester− Fall 2021